Between Lives and Economy: COVID-19 Containment Policy in Open Economies*

Wen-Tai Hsu† Hsuan-Chih (Luke) Lin‡ Han Yang§

March 21, 2023

Abstract

This paper studies containment policies for combating a pandemic in an open-economy context. It does so via quantitative analyses using a model that incorporates a standard epidemiological compartmental model in a general equilibrium multi-country, multi-sector Ricardian model of international trade with input-output linkages. We quantitatively evaluate the long-run welfare and real-income losses due to the short-run pandemic shocks, and we study the role of trade in these effects. We devise a novel approach to computing national optimal policies. We find that (1) the long-run welfare and real-income losses due to just two years of pandemic shocks are substantial; (2) international trade helps buffer both the welfare and real-income losses, and it also saves lives; (3) the computed optimal policies indicate that most countries should have tightened their containment measures relative to what was done; and (4) compared to the case of autarky, the optimal policy under trade is generally more stringent.

Keywords: COVID-19, pandemic, welfare analysis, disease dynamics, effective reproduction number, optimal containment policy, open economy, trade

JEL Classification: I18; F11; F40; E27

*For helpful comments, we thank Ippei Fujiwara, Taiji Furusawa, Matt Shapiro, Michael Zheng Song, and seminar participants in Asia Pacific Trade Seminars, Academia Sinica, Singapore Management University, and the Virtual East Asia Macroeconomic Seminar Series. The online appendix to this paper is available at http://wthsu.com.

†Institute of Economics, Academia Sinica, Taiwan. Email: wthsu@econ.sinica.edu.tw.

‡Institute of Economics, Academia Sinica, Taiwan. Email: linhc@econ.sinica.edu.tw.

§Institute of Economics, Academia Sinica, Taiwan. Email: hanyang@econ.sinica.edu.tw.

1 Introduction

One of the most important questions in a major pandemic, such as the most recent COVID-19 event, is how stringent the containment policies should be. There has been heated debate on this in many countries, and a large cross-country variation in the stringency of containment policies is apparent. The key trade-off is obvious: lives vs. economy. But striking the right balance is not a simple task due to the complexity of the economy and its complicated interaction with the disease's epidemiological evolution. There has been a surge of research on containment policy in macroeconomics literature, but these studies are mostly, if not all, in closed-economy contexts. As the global economy is interlinked across countries, a country's containment policy may have repercussions on other countries' economies through various trade linkages, which may, in turn, affect the considerations of other countries' containment policies and the ensuing health outcomes.

This paper attempts to answer questions regarding containment policy in an open-economy context. We do so by conducting quantitative analyses using a model that incorporates a standard epidemiological compartmental model (**S**usceptible-**I**nfected-**R**ecovered-**D**eceased; SIRD) in a multi-country, multi-sector Ricardian model of international trade with input-output linkages. In particular, our model builds on that of Caliendo and Parro (2015)[1] by adding how the pandemic shocks different sectors and countries differently due to the heterogeneity in containment policy and work-from-home (henceforth WFH) capacity, which in turn reshapes comparative advantages and the distribution of sectoral employment. The rate of disease transmission is then influenced by such changes in sectoral employment through workplace interactions, and the SIRD law of motion then influences the next-period labor supply. Thus, this model features two-way dynamic influences between the economy and the pandemic. It also features cross-country externality of containment policies through trade linkages.

Our welfare measure for a country is the sum of the expected utilities of individuals in that country, where the expected utility is evaluated on an infinite time horizon, following the standard dynastic assumption in macroeconomics. Individuals are concerned with risks in a pandemic, as, ex-ante, no one knows how he/she will fare during the pandemic. With risk aversion, people dislike extreme outcomes; hence, an increase in the probability of death or infection worsens welfare beyond the loss of real income. We intentionally leave out the psychological cost of mortality, as it is difficult to calibrate; in most cases, the direction of changes in optimal policies can be easily predicted when this cost is incorporated. In short, this paper aims to gauge the effect of short-run shocks due to the pandemic from a long-run perspective. The short-run shocks

[1] Caliendo and Parro (2015) extend the Ricardian model of Eaton and Kortum (2002) by adding input-output linkages.

affect the long-run welfare in three ways: (1) by lowering the effective labor supply, (2) by creating temporary shifts in comparative advantages, and (3) by losing population due to deaths caused by the pandemic. The former two ways are short-run effects on the economy, whereas the third way is long-run consequences. But all of these are evaluated in terms of long-run welfare.

We calibrate our model to the pre-COVID-19 economy mainly by using the World Input-Output Database (WIOD), in which there are 41 countries. Our key disease transmission parameters are disciplined by the data on the total deaths from COVID-19. Using the calibrated model, we conduct various counterfactual analyses. In our simulations, we assume that the pandemic ends in two years from January 1, 2020. This is mainly because the pandemic situation drastically eased after Omicron became the dominant variant and because most countries adopted "living with COVID" policies in 2022. See Section 3.2 for a detailed justification.

Our analysis consists of two parts. In the first part, we analyze the effects of the COVID-19 pandemic on welfare and real income and investigate the role of international trade in these effects. In the second part, we study optimal containment policies and examine the role of international trade in determining these policies. The first finding in the first part is that the cross-country weighted averages of real-income losses and welfare losses are 2.73% and 2.34%, respectively. As the losses are measured in terms of the discounted sums on an infinite time horizon, such losses due to only two years of the pandemic are substantial. We also find that larger countries tend to suffer more and that there is a larger cross-country variation in welfare losses than that in real-income losses.

To highlight the role of trade, we compare the losses in welfare and real income during the pandemic under the benchmark model with those under autarky. Our results show that with international trade, the weighted averages of welfare and real-income losses are both smaller than the case under autarky. However, not all countries benefit from trade, as 7 out of 41 countries actually suffer from higher losses with trade than under autarky. Despite trade being a more efficient scheme than autarky, the system of trade can worsen a country's real-income loss if its terms of trade worsen significantly during the pandemic. With respect to health outcomes, we find that the cumulative numbers of confirmed cases and deaths are smaller with trade than in autarky, implying that trade can help the countries to "*flatten the curve*". The reason is that while the country-sector pairs with relatively higher WFH capability expand during the pandemic, trade amplifies the expansions further through international specialization. On average, the weights of the sectors with high WFH capacities in both consumption and production increase. As a result, people are on average less likely to work onsite, and the disease is less likely to spread via face-to-face interaction in workplaces.

In the second part, which concerns optimal containment policies, our key challenge is to

devise a reasonable and tractable approach to reduce the space of candidate policies in such a multi-country, multi-sector, multi-period framework with input-output linkages. To facilitate efficient computation of optimal policies, we use the effective reproduction number R_e as each country's policy target instead of optimizing the entire time paths of containment policies for all countries. The effective reproduction number is a reasonable target because it reflects the speed of disease spread and is the central concern for epidemiologists and doctors who lead government responses. Targeting effective reproduction numbers also implies that containment measures should be stringent initially and generally become more lenient over time, which is consistent with recent findings in the macroeconomic literature.

To further reduce the computational burden, we compute optimal policies in two steps. In the first step, we consider a global planner who seeks to maximize global welfare by deciding on an R_e that applies to all countries. The result from this step serves as the starting point to compute the optimal policies for each country in the second step. In the second step, we solve each country i's optimal effective reproduction number $R_{e,i}$, given other countries' optimal choices $R_{e,-i}$; this is, indeed, a Nash equilibrium of national optimal policies. Information from the first step helps to ease the computational burden in this step as it suggests how the grid search can be efficiently conducted.

Our result indicates that for all countries except China, the optimal $R_{e,i}$'s are less than their corresponding average $R_{e,i}$'s in the benchmark model. This means that for most countries, the containment measures should be stricter than those actually adopted. Moreover, the optimal $R_{e,i}$'s so computed should be interpreted as the upper bounds because we intentionally leave out the psychological cost of mortality. Once this cost is incorporated, optimal effective reproduction numbers should be even smaller; hence the containment measures should be even stricter. For the role of international trade in determining optimal containment policies, we find that most countries' optimal containment policies are stricter under trade than the case under autarky. This result is intuitive because international trade helps buffer real-income losses such that countries can implement stricter containment measures without significantly reducing real consumption.

We conduct a series of sensitivity analyses, including the effects of capital (and trade imbalances), input-output linkages, income support programs, and epidemiological parameters. We find that incorporating capital significantly dampens welfare and real-income losses, as it substantially reduces the effects of labor and hence containment measures. The benchmark results on welfare and real-income losses and the role of trade remain relatively robust to the consideration of input-output linkages, income support programs, and epidemiological parameters.

Related literature. There has been a surge of research studying optimal containment policies:

these studies embed variants of the classic SIR model proposed by Kermack et al. (1927) into macroeconomic models to study various aspects of the tradeoff between lives and economy. See, for example, Acemoglu et al. (2021), Alvarez et al. (2021), Atkeson (2020), Atkeson et al. (2021), Eichenbaum et al. (2021), Farboodi et al. (2021), Jones et al. (2021), Krueger et al. (2022), and Piguillem and Shi (2023). Our work differs from these in our focus on analyzing optimal containment policies in an open-economy context. A particularly closely related work is that by Budish (2020), who formulates a static optimization problem using $R_e < 1$ as a constraint. Our work differs as R_e is used as a policy target (rather than a constraint) in a dynamic setting.

Also closely related are the studies by Antràs et al. (2023), Fajgelbaum et al. (2021), and Argente et al. (2021), all of whom consider disease dynamics in a general equilibrium model of trade in either a city or an international-trade setting. Our work differs from Antràs et al. (2023) mainly due to our focus on optimal containment policies, and it differs from Fajgelbaum et al. (2021) and Argente et al. (2021) due to our focus on country-level containment policies. Our work is also related to Chen et al. (2020), Bonadio et al. (2021), Eppinger et al. (2020), and Sforza and Steininger (2020), as both our work and these studies evaluate the economic consequences of the pandemic shocks and study the role of trade and/or input-output linkages. However, these studies do not incorporate disease dynamics or analyze optimal containment policies, which are our main contributions relative to these studies.

As our model and counterfactual analyses are already complex with the computation of national optimal policies in a setup with multiple countries, multiple sectors, input-output linkages, trade imbalances, and disease dynamics, it is rather burdensome to account for other dynamic aspects. As mentioned above, this paper should be read as gauging the effects of short-run shocks due to the pandemic from a long-run perspective. We leave out long-run dynamic aspects to isolate these effects. For these aspects, readers may be referred to Chernoff and Warman (2022) and Gordon and Sayed (2022) for the effects of the pandemic on technological changes and Hsu et al. (2022) and Kozlowski et al. (2020) for the long-lasting effects of scarred beliefs.

The rest of the paper is organized as follows. Section 2 describes the model; Section 3 introduces the data and how the model is calibrated; Section 4 presents the quantitative analyses of the effects of the pandemic and studies optimal containment policies; Section 5 concludes.

2 Model

Our model incorporates the evolution of the pandemic and the labor productivity shocks arising from the pandemic into a general equilibrium Eaton and Kortum (2002) model with multiple sectors.

2.1 Preference

There are K countries, each of which has an initial population of $N_i, i \in \{1, 2, ..., K\}$. There are J sectors, each of which consists of a unit continuum of varieties. The final-good consumption of an individual in country i in period t, $q_{i,t}$, consists of a Cobb–Douglas bundle of sectoral goods:

$$q_{i,t} = \prod_{j=1}^{J} (q_{i,t}^{F,j})^{\alpha_i^j},$$

and each sectoral good $q_{i,t}^{F,j}$ is made of a CES composite:

$$q_{i,t}^{F,j} = \left[\int_0^1 q_{i,t}^{F,j}(\omega)^{\frac{\kappa-1}{\kappa}} d\omega \right]^{\frac{\kappa}{1-\kappa}}, \tag{1}$$

where $q_{i,t}^{F,j}(\omega)$ is the amount of variety ω used for final consumption and $\kappa > 1$ is the elasticity of substitution. The lifetime utility of an individual (in a dynastic sense) is given by

$$u_i = \sum_{t=0}^{\infty} \rho^t u\left(q_{i,t}\right),$$

where ρ is the discount factor and u is a concave and strictly increasing function.

2.2 Production

Labor and capital are the fundamental inputs for production, and the production in each sector potentially uses intermediate inputs from all sectors. Countries differ in their productivities across sectors and varieties. Production technology exhibits constant returns to scale. Both the goods and factor markets are perfectly competitive.

Let $M_{i,t}^j(\omega)$ denote the use of the composite intermediate goods by the firms producing variety ω in sector j and country i; it is made of a Cobb–Douglas composite:

$$M_{i,t}^j = \prod_{l=1}^{J} (q_{i,t}^{M,l})^{\gamma_i^{j,l}}, \tag{2}$$

where the sectoral good $q_{i,t}^{M,l}$ is made by the same CES aggregator across varieties as in (1) with the inputs being $q_{i,t}^{M,j}(.)$. Note that each sector j's intermediate composite's expenditure share on sector l's good, $\gamma_i^{j,l}$, is country-specific.

Denote a country-sector-time-specific pandemic shock parameter on the production function by $B_{i,t}^j$, which will be specified later; for the pre-COVID-19 economy, this term drops out as $B_{i,t}^j = 1$. The production function of a variety ω in sector j and country i is given by

$$y_{i,t}^j(\omega) = \frac{z_i^j(\omega) \left[B_{i,t}^j L_{i,t}^j(\omega)\right]^{\beta_i^{L,j}} \left[K_{i,t}^j(\omega)\right]^{\beta_i^{K,j}} M_{i,t}^j(\omega)^{1-\beta_i^{L,j}-\beta_i^{K,j}}}{(\beta_i^{L,j})^{\beta_i^{L,j}} (\beta_i^{K,j})^{\beta_i^{K,j}} (1-\beta_i^{L,j}-\beta_i^{K,j})^{1-\beta_i^{L,j}-\beta_i^{K,j}}}, \tag{3}$$

where $L_{i,t}^j(\omega)$ and $K_{i,t}^j(\omega)$ are the labor and capital hired for this variety and the Hicks-neutral productivity $z_i^j(\omega)$ is drawn *i.i.d.* from a Fréchet distribution: $\Pr(x < z) = \exp(-T_i^j z^{-\theta})$, where $T_i^j > 0$ is the country-sector-specific scaling parameter and $\theta > 1$ is the shape parameter. The draws are also independent across countries and sectors.

The trade cost is of the standard iceberg-cost form: to deliver one unit of sector-j variety from country i to country n, $\tau_{i,n}^j \geq 1$ units are required to ship. The unit cost of delivering a good from country i to country n is $c_{i,t}^j \tau_{i,n}^j / z_{i,t}^j(\omega)$, where

$$c_{i,t}^j = \left(\frac{w_{i,t}}{B_{i,t}^j}\right)^{\beta_i^{L,j}} (r_{i,t})^{\beta_i^{K,j}} (P_{i,t}^{M,j})^{1-\beta_i^{L,j}-\beta_i^{K,j}}, \tag{4}$$

where $w_{i,t}$ and $r_{i,t}$ are country i's wages and capital rent. Here, $c_{i,t}^j$ is indeed the unit cost to produce a sector j variety under unit productivity. In this environment with perfect competition and constant returns to scale, prices equal the (delivered) marginal costs, and each country n buys from the cheapest source: $p_{n,t}^j(\omega) = \min_i \left\{ c_{i,t}^j \tau_{i,n}^j / z_{i,t}^j(\omega) \right\}$. Standard derivations yield the price indices of the sectoral goods $P_{i,t}^j$, those of the final consumption goods $P_{i,t}$, and those of the sectoral intermediate goods $P_{i,t}^{M,j}$, respectively:

$$P_{i,t}^j = \left(\int_0^1 p_{i,t}^j(\omega)^{1-\kappa} \right)^{\frac{1}{1-\kappa}}, \quad P_{i,t} = \prod_{j=1}^J \left[P_{i,t}^j \right]^{\alpha_i^j}, \quad P_{i,t}^{M,j} = \prod_{l=1}^J (P_{i,t}^l)^{\gamma_i^{j,l}}. \tag{5}$$

2.3 Pandemic and Economy

We incorporate a standard epidemiological model, i.e., an SIRD model, as follows. At any period t, the population of country i, N_i, consists of people who are **S**usceptible ($S_{i,t}$, have not been exposed to the disease), **I**nfectious ($I_{i,t}$, have contracted the disease), **R**ecovered ($R_{i,t}$, have recovered and are immune), and **D**eceased ($D_{i,t}$, died from the disease). As we abstract away from population growth, $N_i = S_{i,t} + I_{i,t} + R_{i,t} + D_{i,t}$. The epidemiology is characterized by

$$\begin{aligned}
S_{i,t+1} &= S_{i,t} - T_{i,t} + \pi^s R_{i,t} \\
I_{i,t+1} &= I_{i,t} + T_{i,t} - (\pi^r + \pi_{i,t}^d) I_{i,t} \\
R_{i,t+1} &= R_{i,t} + \pi^r I_{i,t} - \pi^s R_{i,t} \\
D_{i,t+1} &= D_{i,t} + \pi_{i,t}^d I_{i,t},
\end{aligned}$$

where π^r and $\pi_{i,t}^d$ are the probabilities of recovering and dying from the infectious state, respectively, π^s is the probability of losing immunity for the recovered, and $T_{i,t}$ is the number of newly infected people. To capture the fact that the strain of the number of infectious people on the medical system generally increases the mortality rate $\pi_{i,t}^d$, we assume $\pi_{i,t}^d = \pi^d + \delta I_{i,t}/N_i$, where

$\delta > 0$ and π^d is the base mortality rate. This linear form is also assumed by Alvarez et al. (2021). Next, we link the SIRD model back to our economic environment. As deaths reduce the labor force and infections negatively affect individuals' labor supply, the effective labor force at time t is

$$L_{i,t} = S_{i,t} + R_{i,t} + \alpha^I I_{i,t}, \tag{6}$$

where a fraction $1 - \alpha^I$ of labor time is lost from contracting the disease.

Let $\mu_i^j \in [0,1]$ be the capacity to work from home for sector j in country i, and let $\eta_{i,t} \in [0,1]$ be the degree of the containment measure in country i at time t; $\eta_{i,t} = 1$ means a total lockdown whereas $\eta_{i,t} = 0$ means totally laissez-faire, but a containment policy can be anywhere in between. Assume that during a pandemic, workers who can work from home (the fraction of such workers is μ_i^j) work from home regardless of the containment policy, but for those workers who are unable to work from home, they must still meet in workplaces if allowed. If a country's containment measure is $\eta_{i,t}$, then a fraction $\eta_{i,t}(1-\mu_i^j)$ of workers are locked away. Only those who are not locked away still meet; the fraction of such workers is $(1-\eta_{i,t})(1-\mu_i^j)$. Assume that the containment measure also applies to interactions in general activities. The number of newly infected individuals is given by

$$T_{i,t} = \frac{(1-\eta_{i,t})\pi_i^I S_{i,t} I_{i,t} + \pi_i^L \times \sum_{j=1}^J \left[(1-\eta_{i,t})(1-\mu_i^j)\ell_{i,t}^j\right] S_{i,t} I_{i,t}}{N_i}, \tag{7}$$

where $\ell_{i,t}^j$ is sector j's employment share in country i at time t, and π_i^L and π_i^I are the infection rates from interactions at workplaces and from general activities other than working, respectively. Similar forms have been used in Eichenbaum et al. (2021) and Jones et al. (2021). The key difference between our study and these macroeconomic models is that instead of focusing on how households react to the pandemic by cutting their consumption and labor supply, we expand in the country and sector dimensions to study how sectoral employment shares $\{\ell_{i,t}^j\}$ react to changing circumstances of containment policies, augmented by the sectoral WFH capacity, and subsequently affect the speed of disease spread.

As the effective labor time supplied per worker in sector j and country i is reduced to $\mu_i^j + (1-\eta_{i,t})(1-\mu_i^j) = 1 - \eta_{i,t}(1-\mu_i^j)$, the employers can pay the full wages even when workers' effective time supplied is reduced or they can choose to lay off workers or hire part-time. In the former case, employers absorb the shocks directly, whereas the workers absorb the shocks in the latter case. Both scenarios are present in reality, and their effects are similar. To keep the model tractable, we focus on the former case. Thus, the pandemic-shock parameter in the production function (3) is $B_{i,t}^j \equiv 1 - \eta_{i,t}(1-\mu_i^j) \in [0,1]$. In the case where $\eta_{i,t} = 0$ (as would be the case when there is no pandemic or when a laissez-faire policy is adopted), $B_{i,t}^j = 1$.

Observing (3) and (7), a more stringent containment measure (higher $\eta_{i,t}$) reduces infections but hurts production; both effects are mitigated if the sector of concern has a larger WFH capacity. Both effects also differ across countries due to the differences in infection probabilities $\{\pi_i^I, \pi_i^L\}$ and country-specific production parameters. The international division of labor reflected by $\{\ell_{i,t}^j\}$ provides an *endogenous source* of cross-country heterogeneity in the rate of transmission. We allow for π_i^I and π_i^L to differ across countries because these may reflect country-specific environments, such as geography, climate, or culture, that potentially affect the rate of disease transmission given the same intensity of interactions in workplaces and in general.

Assuming $\kappa < \theta + 1$, the price index of a sectoral good is given by

$$P_{n,t}^j = \zeta \left[\sum_{k=1}^{K} T_k^j \left(c_{k,t}^j \tau_{k,n}^j \right)^{-\theta} \right]^{-\frac{1}{\theta}}, \tag{8}$$

where $\zeta \equiv \left[\Gamma \left(\frac{\theta+1-\kappa}{\theta} \right) \right]^{1/(1-\kappa)}$, and the expenditure share of sector-j goods that country n purchases from country i is given by

$$\pi_{i,n,t}^j = \frac{T_i^j \left(c_{i,t}^j \tau_{i,n}^j \right)^{-\theta}}{\sum_{k=1}^{K} T_k^j \left(c_{k,t}^j \tau_{k,n}^j \right)^{-\theta}}. \tag{9}$$

Importantly, note that the effect of the pandemic shock $B_{k,t}^j$ is already incorporated in $c_{i,t}^j$ as in (4).

Containment policies combined with WFH capacity create temporary shifts in comparative advantages during the pandemic. If all countries adopt the same containment policy, a country i gains a comparative advantage in those high μ_i^j sectors as the corresponding $B_{i,t}^j$'s are larger. This means that a country's containment policy affects its *own and other* countries' distributions of sectoral employment. Subsequently, their rates of disease spread change, thus affecting the labor supply (and hence wages and comparative advantages) in the next period. Such a cross-country externality of containment policies cannot be captured in a closed-economy model. Moreover, this model is not a Caliendo–Parro model repeatedly shocked by a disease evolution that runs independently. Instead, it features a dynamic mechanism in which the economic situations also change the speed of disease spread.

Here, we can already comment on the potential roles of international trade during the pandemic. First, besides trade being a more efficient scheme, it may dampen the adverse effects of containment measures on the economy because it amplifies the expansion of the WFH sectors, which are less subject to these measures, relative to the expansion in an autarkic world. Second, when the economy shifts its weight toward WFH sectors, the sectoral employment shares $\ell_{i,t}^j$ of these sectors increase. Thus, infections through interactions in workplaces are reduced, as is

evident from the second term in the numerator of (7). Because trade amplifies the expansion of WFH sectors during the pandemic relative to autarky, it is expected to help reduce infections and hence total deaths.

2.4 Equilibrium

Let $R_{i,t}^j$ denote the total revenue of country i's sector j, $X_{n,t}^j$ denote the total expenditure of country n on goods in sector j, and $X_{n,t}$ denote the total expenditure of country n. By definition, $R_{i,t}^j = \sum_{n=1}^K \pi_{i,n,t}^j X_{n,t}^j$. The labor and capital market clearing conditions are therefore

$$w_{i,t}L_{i,t} = \sum_{j=1}^J \beta_i^{L,j} R_{i,t}^j = \sum_{j=1}^J \sum_{n=1}^K \beta_i^{L,j} \pi_{i,n,t}^j X_{n,t}^j \tag{10}$$

$$r_{i,t}K_{i,t} = \sum_{j=1}^J \beta_i^{K,j} R_{i,t}^j = \sum_{j=1}^J \sum_{n=1}^K \beta_i^{K,j} \pi_{i,n,t}^j X_{n,t}^j. \tag{11}$$

Following Caliendo et al. (2019), we incorporate the observed trade imbalance. In each country i, local capital is owned by immobile rentiers, and rentiers send all rents to a global portfolio and then receive a fixed share φ_i from the global portfolio. Let $Y_{i,t}$ be the total income of country i at time t, satisfying

$$Y_{i,t} = w_{i,t}L_{i,t} + \varphi_i \sum_{n=1}^K r_{n,t}K_n. \tag{12}$$

By the definition of $X_{i,t}^j$, producers also spend shares of costs in purchasing intermediate inputs from various sectors; total expenditure $X_{i,t}^j$ is given by

$$X_{i,t}^j = \alpha_i^j Y_{i,t} + \sum_{l=1}^J \sum_{n=1}^K \gamma_i^{l,j}(1 - \beta_i^{L,l} - \beta_i^{K,l})\pi_{i,n,t}^l X_{n,t}^l. \tag{13}$$

Note that in this model with trade imbalances, the total revenue of a country may differ from its total income, which is its total expenditure on final goods. Thus, a country has a trade deficit if its total income $Y_{i,t}$ is larger than its total revenue ($\sum_{j=1}^J R_{i,t}^j$) net of its total purchases on intermediate inputs (the second term on the right-hand side of [13]).

A brief description of the equilibrium algorithm is given as follows; the detailed algorithm is relegated to the online appendix.[2] We first solve the equilibrium at time t given the SIRD objects $\{S_{i,t}, I_{i,t}, R_{i,t}, D_{i,t}\}$ and $\{L_{i,t}\}$ from (6). Given wages and rental prices of capital $\{w_{i,t}, r_{i,t}\}$, $\{c_{i,t}^j, P_{i,t}, P_{i,t}^j, P_{i,t}^{M,j}, \pi_{i,n,t}^j, X_{k,t}^j\}$ are obtained from (4), (5), (8), (9), and (13). Equilibrium wages and rental prices of capital are obtained from (10) and (11). In particular, sectoral employment shares are computed by $\ell_{i,t}^j = \beta_i^{L,j} R_{i,t}^j / \left[\sum_{l=1}^J \beta_i^{L,l} R_{i,t}^l\right]$. Then, the next-period SIRD objects are

[2]The online appendix is available at https://wthsu.com.

obtained from the law of motion specified in Section 2.3 with the number of newly infected $\{T_{i,t}\}$ given by (7).

2.5 Welfare

A pandemic poses uncertainty to individuals as to how one will fare in terms of the compartments $\{S_{i,t}, I_{i,t}, R_{i,t}, D_{i,t}\}$. For a country i, its welfare is measured by the sum of individual expected lifetime utility in which everyone's probability of falling into each compartment is given by the fraction of people in that compartment. Note that this probability is unconditional when viewed at time 0.

The welfare of country i is given by

$$U_i = \sum_{t=0}^{\infty} \rho^t \left[(S_{i,t} + R_{i,t})\, u\left(\frac{w_{i,t} + b_{i,t}}{P_{i,t}}\right) + I_{i,t} u\left(\frac{\alpha^I w_{i,t} + b_{i,t}}{P_{i,t}}\right) + D_{i,t} u\,(0) \right], \tag{14}$$

where

$$b_{i,t} = \frac{\varphi_i \sum_{n=1}^{N} K_{n,t} r_{n,t}}{S_{i,t} + R_{i,t} + I_{i,t}}$$

is country i's capital income per capita. Note that the concavity of u reflects the degree of risk aversion. This formulation treats an individual's death as a complete loss of labor, which implies zero income and hence zero consumption. If $u(0) = 0$, then the loss from death is simply the loss of utility from the other two outcomes before one's death. When $u(0) \neq 0$, its value actually reflects the psychological cost that one may have toward death. As it is difficult to calibrate psychological costs, we set $u(0) = 0$ for a relatively clear benchmark. In most cases, it is easy to predict the direction of how our results change when psychological costs are incorporated. When u is linear, i.e., the risk-neutral case, a country i's welfare actually becomes the present value of aggregate real income: $U_i = \sum_{t=0}^{\infty} \rho^t \frac{w_{i,t} L_{i,t} + \varphi_i \sum_{n=1}^{N} K_{n,t} r_{n,t}}{P_{i,t}}$.

The global welfare is defined analogously:

$$\begin{aligned} U &= \sum_{i=1}^{K} U_i \\ &= \sum_{i=1}^{K} \sum_{t=0}^{\infty} \rho^t \left[(S_{i,t} + R_{i,t})\, u\left(\frac{w_{i,t} + b_{i,t}}{P_{i,t}}\right) + I_{i,t} u\left(\frac{\alpha^I w_{i,t} + b_{i,t}}{P_{i,t}}\right) + D_{i,t} u\,(0) \right]. \end{aligned} \tag{15}$$

As U_i is already the aggregate welfare that takes into account the population in country i, the global welfare is simply the sum of individual countries' welfare.

3 Calibration

This section describes how we quantify the model. We first present the calibration for the international trade model and then discuss how to calibrate the epidemiological parameters. More details of the quantification are relegated to Appendix A.

3.1 Economic Parameters

For our quantitative analyses, we set the per-period utility as

$$u(q) = \frac{(q+1)^{1-\sigma} - 1}{1-\sigma}.$$

We choose this functional form for three reasons. First, this specification is similar to the CRRA (constant relative risk aversion) utility if the term $q + 1$ is replaced with q. Thus, it is approximately CRRA when q is large; the parameter σ measures the degree of relative risk aversion. Second, $u(0) = 0$, which satisfies our requirement to leave psychological costs out of the model; note that the exact CRRA utility entails $\lim_{q\to 0} u(q) \to -\infty$ when $\sigma \geq 1$ and is therefore not implementable. Third, $\sigma = 0$ corresponds to the risk-neutral case. Following Low and Pistaferri (2015), the relative risk aversion σ is set to 1.5. Following Farboodi et al. (2021), we set the annual discount factor as 0.95. Therefore, the daily discount factor is $\rho = 0.95^{\frac{1}{365}} \approx 0.99986$. As will be explained below, we will simulate the economic module of the model at a quarterly frequency; thus, in our computation, the economic module repeats for 90–92 days with the daily discount factor being applied.

The economic environment is calibrated to the world economy prior to the COVID-19 pandemic using the World Input-Output Database (WIOD) and Centre d'Études Prospectives et d'Informations Internationales (CEPII) data. There are 41 countries in this data set. We aggregate the 56 WIOD industries into six sectors (one primary sector, three manufacturing sectors, and two service sectors distinguished by high skill and low skill). Hence, $K = 41$ and $J = 6$.

The share parameters $\{\alpha_i^j\}$ in the utility and production functions are calibrated using the input-output information in the WIOD. With data on total capital compensation for each country from the Social Economic Account (SEA) in the WIOD, the country-specific portfolio shares $\{\varphi_i^j\}$ are calibrated to fit trade imbalances. Given the data on trade shares and geography from the WIOD and CEPII, the model's gravity equations and hence trade costs $\{\tau_{i,n}^j\}$ can be estimated. Following Simonovska and Waugh (2014), we set the value of trade elasticity $\theta = 4$. Given trade elasticity, estimated trade costs, the share parameters $\{\alpha_i^j\}$, and data on wages obtained from the SEA, the productivity parameters $\{T_i^j\}$ can then be backed out using the model structure, as in Fieler (2011) and Ravikumar et al. (2019).

The values of WFH capacity $\{\mu_i^j\}$ are obtained from Dingel and Neiman (2020), who compute such capacity by occupation and then aggregate to NAICS industries. We map their 3-digit NAICS results to WIOD industries and our aggregate sectors. The containment measures $\{\eta_{i,t}\}$ are obtained from the *Stringency Index* of the Oxford COVID-19 Government Response Tracker (OxCGRT; Hale et al. 2020) at a daily frequency. This index summarizes a government's responses in terms of various closures and containment measures, including school and workplace closures, stay-at-home requirements, border control, and restrictions on gatherings, public events, public transport, and internal movements, as well as public information campaigns.

3.2 Epidemiological Parameters

Next, we turn to the epidemiological parameters $\{\pi^r, \pi^d, \pi^s, \delta, \pi_i^I, \pi_i^L, \alpha^I, I_{i,0}\}$. Note that recovery rate π^r, death rate π^d, reinfection rate π^s, medical preparedness δ, and reduction in productivity α^I are the same across countries, while π_i^I and π_i^L, the infection rates from workplace and general activities, are country-specific. We now describe how these parameter values are set.

For the parameter values that are the same across countries, we follow the choices in the literature. As in Atkeson (2020) and several other macro-SIRD models, we set $\pi^r + \pi^d = 1/18$, which means that it takes on average 18 days to either recover or die from the infection. The case mortality rate is set at $\pi^d = 0.016 \times \frac{1}{18}$. According to Helfand et al. (2022), we set $\pi^s = 0.476\%$. Following Alvarez et al. (2021), we set $\delta = 0.05 \times \frac{1}{18}$. As a WHO (2020) COVID-19 Situation Report indicates that asymptomatic and mild cases account for about 80% of the infections, we set $\alpha^I = 0.8$.

As for parameters that are country-specific, we describe how to calibrate them. For our purpose, it is important to account for the variations in the rate of disease reproduction across countries, the key parameters for which are the two infection probabilities $\{\pi_i^I, \pi_i^L\}$ in (7). Also, for the epidemiological evolution to commence, an estimate of $I_{i,0}$ is required (as $S_{i,0} = N_i - I_{i,0}$ and $R_{i,0} = D_{i,0} = 0$); $I_{i,0}$ is generally unknown and must be estimated because the society might be unaware of, unprepared for, or on low alert for the disease so that the number of the first few reported cases may be quite off. From the SIRD module of the model, we can simulate daily time series of the cumulative total death for each country during the pandemic. The time period of the pandemic is set to be the entire two years of 2020 and 2021, the reasons for which will be explained shortly. For each country, parameters $\{\pi_i^I, \pi_i^L, I_{i,0}\}$ are estimated by the non-linear least squares method that minimizes the sum of squared distance in the cumulative total deaths between data and model. The data on total deaths is downloaded from the Humanitarian Data Exchange website.[3] Our estimated model fits the data reasonably well, as the cross-country av-

[3]See Dong et al. (2020) (`https://data.humdata.org/dataset/novel-coronavirus-2019-ncov-cases`) for data.

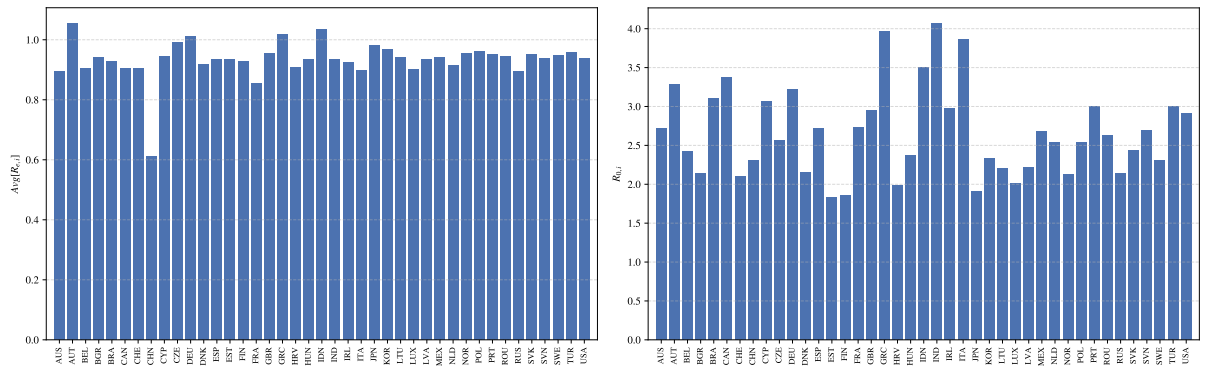

(a) Average Effective Reproduction Number $\bar{R}_{e,i}$ (b) Calibrated Basic Reproduction Number $R_{0,i}$

Figure 1: Effective Reproduction Number $\bar{R}_{e,i}$ and Basic Reproduction Number $R_{0,i}$

erage of the normalized root-mean-square deviation (NRMSD, which is an inverse measure of model fit) is 0.25 (the average R^2 is 0.87).

Note that we choose to match the total deaths over time because the numbers of total confirmed cases are noisier and do not fully reflect actual total infections. We have a calibrated version that is based on the total confirmed cases, and the results are qualitatively similar. Also, note that cultural and institutional factors may simultaneously affect the two infection rates. Even though, theoretically, the two infection rates π_i^L and π_i^I are independent, our calibration strategy already connects the two infection rates tightly, because we borrow the results in Eichenbaum et al. (2021) and assume that $1/3$ of the infections come from workplaces and $2/3$ from general activities. Thus, both calibrated rates are higher for a country with more infections and deaths.

We regard the pandemic period as the two years from January 1, 2020 to the end of 2021. The reasons are mainly three-fold. First, the Omicron variant, which is much more contagious than the previous strains and hence replaces them, is much less lethal. The Omicron variant was discovered in South Africa in early November 2021 and spread to the entire world in two months. Second, various cures became available around late 2021 and early 2022.[4] Third, mass vaccinations and cumulative infections have helped establish certain degrees of immunity. Due to these reasons, most countries have adopted a "living with COVID-19" policy and abolished most containment measures.

3.3 Reproduction Numbers and Model Fits

We now discuss certain implications of the calibration that are of interest. First, note that a key object in epidemiology is the effective reproduction number $R_{e,i,t}$, which is the number of cases

[4]For example, Paxlovid was authorized in the US and EU in December 2021 and January 2022, respectively.

directly generated from one case, is given by

$$R_{e,i,t} \equiv \frac{T_{i,t}}{I_{i,t}} \times 18 = (1-\eta_{i,t}) \left[\pi_i^I + \pi_i^L \times \sum_{j=1}^{J} (1-\mu_i^j) \ell_{i,t}^j \right] \times 18 \times \frac{S_{i,t}}{N_i}. \tag{16}$$

To further understand the significance of $R_{e,i,t}$, note that the expression in brackets is actually the rate of transmission (the rate of getting infected from susceptible people); when this rate is divided by the rate of leaving the infectious compartment, $1/18$, it entails the number of cases directly generated from one case at the onset of the disease and without government intervention (so $S_{i,t}/N_i = 1$ and $1 - \eta_{i,t} = 1$). This is actually the famous basic reproduction number R_0, although in our model it is actually country-specific and time-varying (denoted as $R_{0,i,t}$) due to cross-country differences in $\{\pi_i^I, \pi_i^L \, \ell_{i,t}^j\}$ and the time variability in $\ell_{i,t}^j$. Then, the effective number of cases generated directly from one case is the product of $R_{0,i,t}$ and the fraction of "effective" susceptible people given by $(1-\eta_{i,t})S_{i,t}/N_{i,t}$.

From (16), it is easy to understand two main strategies for combating the disease. One approach is to impose sufficiently stringent containment measures so that the effective reproduction number goes below 1, in which case the disease spread slows down, and to wait for vaccines. The second approach is to use various ways to "protect the vulnerable" while letting the disease spread faster in the hope of herd immunity. In the first approach, $1 - \eta_{i,t}$ remains low, but the fraction of susceptible in the population remains high; this approach would not be feasible without reasonable prospects for vaccines in the near future. In the second approach, $1 - \eta_{i,t}$ is high, but $S_{i,t}/N_i$ goes down faster and when $S_{i,t}/N_i$ is so low that $R_{e,i,t} < 1$ even when there is no containment measure ($\eta_{i,t} = 0$), herd immunity is reached.

Figure 1 shows the over-time average of both $R_{0,i,t}$ and $R_{e,i,t}$ for each country. There is considerable cross-country variation in the basic reproduction number, ranging from slightly below 2 to slightly above 4. However, when it comes to the effective reproduction number, the variation is much smaller. Most importantly, the scale of average $R_{e,i,t}$ is much smaller than that of average $R_{0,i,t}$, with the former being close and slightly below 1 for most countries. This indicates a strong containment effort from governments across the globe to slow the spread of the disease.

Finally, we demonstrate the model fit of the economic side of our calibration. As one of the main goals is to study the role of international trade, it is important to check whether our model does a reasonable job of matching the observed cross-section of trade shares. Figure 2 plots bilateral trade shares generated using the model against those observed in the data. The NRMSD is 0.17. This suggests that our model captures pre-pandemic trade flows reasonably well.

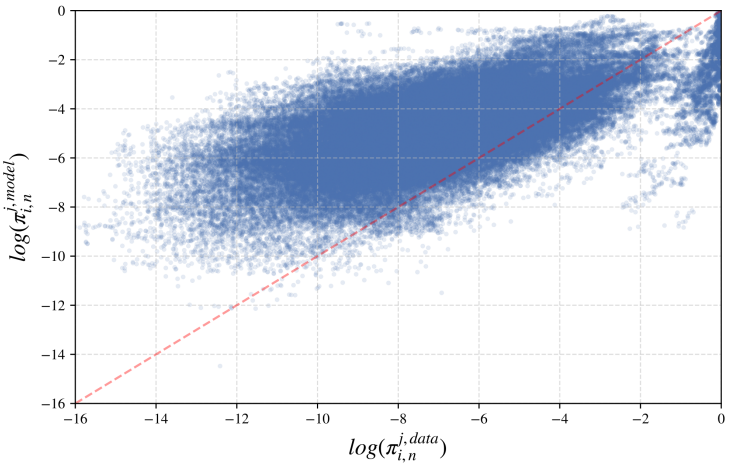

Figure 2: Bilateral Trade Fit

4 Counterfactual Experiments

Using the calibrated model, this section conducts a series of counterfactual experiments, focusing on (1) the effects of pandemic shocks, (2) the role of international trade in such effects, (3) optimal containment policies, and (4) the role of international trade in determining optimal policies.

We now describe the simulation environment. The economy starts on January 1, 2020 ($t = 0$), at the pre-COVID-19 state. Assume that the disease for a country i starts at the date on which the total confirmed cases in the data exceed 50; this date is denoted as t_i^*. Then, the estimated $I_{i,0}$ is applied to the previous day ($t_i^* - 1$); for all days between January 1, 2020 and that previous day, $I_{i,t} = R_{i,t} = D_{i,t} = 0$ and $S_{i,t} = N_{i,t}$. From date t_i^*, the disease evolution follows the law of motion described in Section 2.3.

While we simulate the disease evolution daily, the economy is simulated quarterly to capture the fact that labor adjustment across sectors takes time. Let $\eta_{i,Q}$ denote the average of $\{\eta_{i,t}\}_{t \in Q}$ for quarter Q. Then, the pandemic shock $B_{i,Q}^j = 1 - \eta_{i,Q}(1 - \mu_i^j)$ is fed into the model quarterly. While $L_{i,t}$ evolves daily according to the laws of motion in Section 2.3, $L_{i,Q}$ as the quarterly average of $L_{i,t}$ for $t \in Q$ is fed into the economic module of the model.

As discussed in Section 3.3, we assume the pandemic ended at the end of 2021. For dates after January 1, 2022, we let $\pi_i^N = \pi_i^I = 0$; thus the effective reproduction number also becomes zero. Containment measures are also scrapped from January 1, 2022. Note that the disease evolution does not immediately end at $t = 730$, as it takes some time for infectious people to move to the next state (recovery or death). Therefore, the global economy will gradually move toward a new steady state, in which each country has fewer people than in the pre-COVID economy. We simulate the evolution of the economy until the end of 2022 to ensure the economy is close to the new steady state. For the welfare for the periods since 2023, the net present value is taken at the

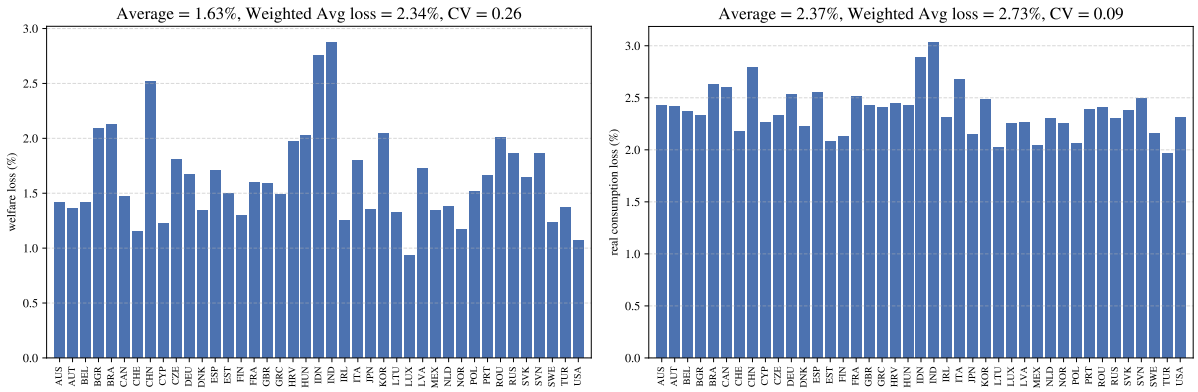

(a) Welfare Losses

(b) Real-Income Losses

Figure 3: Welfare and Real-Income Losses under Trade

beginning of 2023.

4.1 Welfare and Income Losses Due to the Pandemic in the Global Economy

We first examine the losses in welfare and real income due to the pandemic shocks by comparing the economy under these shocks (which are inclusive of the disease dynamics, containment policies, and WFH capacity) with an economy that runs as if there were no such shock from January 1, 2020 to the end of 2021. In Figure 3, the x-axis contains country labels, and the percentage change (loss) compared to the case without a pandemic is on the y-axis. The shorter the bar, the less impact this pandemic has.

The simple and population-weighted averages of losses in real income are 2.37% and 2.73%, respectively. Recall that the losses are measured in terms of the discounted sums when time is taken to infinity as in (B.5); thus such losses due to only two years of the pandemic are substantial. As the weight is by population, this difference in the two averages indicates that large countries suffer more in general; this is also clear from the figure. The simple and population-weighted averages of the welfare losses are 1.63% and 2.34%, respectively. Again, larger countries tend to suffer more. The variation in welfare loss is larger than that in real-income losses; the coefficients of variation are 0.26 and 0.09, respectively. Because risk-averse agents prefer smoother consumption paths, the cross-country differences in time volatility of these paths induce a larger variation in welfare loss than in real-income loss. In addition, a poor country's welfare loss for the same real-income loss is larger than a rich country's because of decreasing marginal utility under a concave utility function. Thus, cross-country income differences may also contribute to the larger variation in welfare losses.

Next, we examine the role of international trade in the above-analyzed effects. We are interested in knowing whether trade mitigates or amplifies the losses from COVID shocks. To

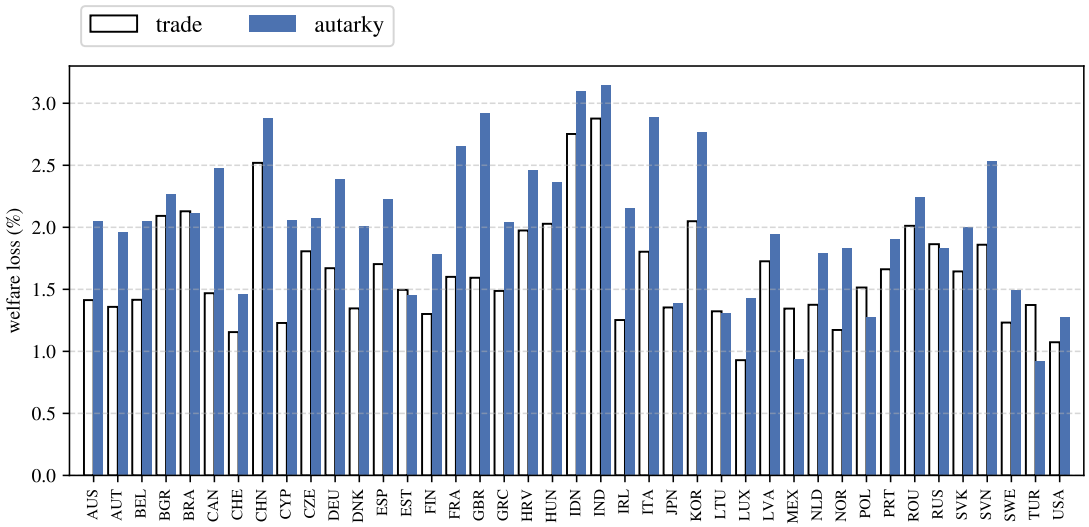

(a) Welfare Losses (%) Between Trade and Autarky

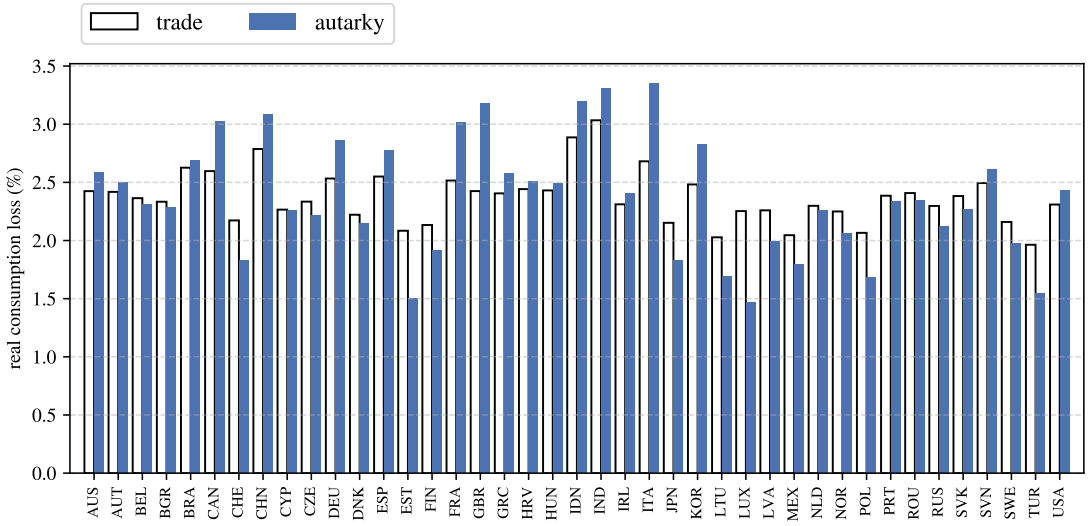

(b) Real-Income Losses (%) Between Trade and Autarky

Figure 4: Welfare and Real-Income Losses: The Role of Trade

highlight the role of trade, we compare the above results from the benchmark model with those from the model where all countries are in autarky. The weighted average of welfare and real-income losses under autarky are 2.64 and 2.95, respectively. These numbers are larger than those under trade (2.73% and 2.34%), indicating that trade mitigates the losses from the pandemic shocks, overall speaking. There exist large cross-country variations, as seen in Figures 4a and 4b. Among 41 countries, 34 countries have a smaller welfare loss under trade than under autarky, while 19 have a smaller real-income loss under trade than under autarky. Despite trade being a more efficient scheme than autarky, the system of trade can worsen a country's real-income loss if its terms of trade worsen significantly during the pandemic. Nevertheless, trade mitigates

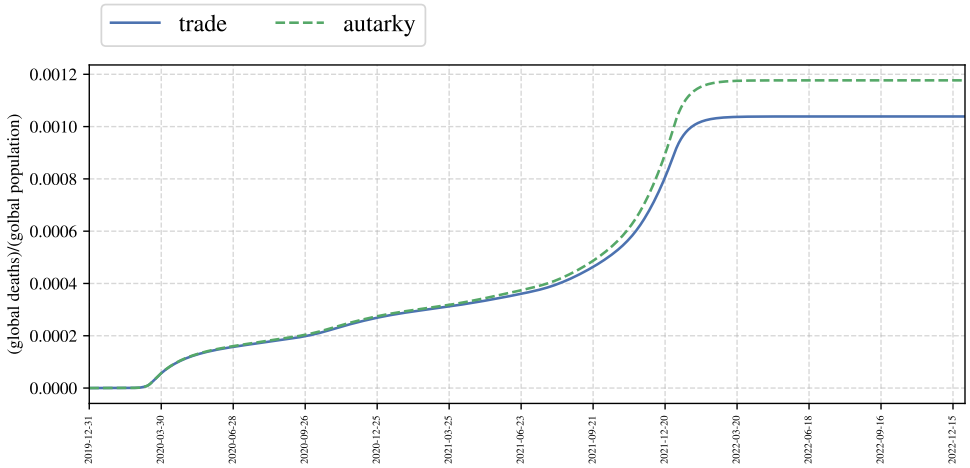

Figure 5: Total Deaths

Figure 6: Cumulative Deaths Between Trade and Autarky Over Time

welfare losses for a majority of countries because it smooths the time path of real income (which is real consumption).

Last, we consider whether and how trade mitigates or amplifies the health impact of the pandemic. Figure 6 presents the total deaths over time under trade (plotted using a dashed line) and in autarky (plotted using a solid line).[5] Clearly, there are fewer total deaths under trade than under autarky. Trade reduces the number of total deaths by 11.7%. The intuition is as follows. The pandemic shocks differ across countries and sectors, and thus they create temporary shifts in comparative advantages. Our model shows that a country-sector pair becomes relatively more competitive during the pandemic if it had a greater WFH capacity and less stringent containment measures. Trade amplifies these new competitive edges. Hence, while country-sector pairs with relatively higher WFH capability expand during the pandemic, trade amplifies the expansions even further. Through trade and international specialization, people, in general, are less likely to work onsite; as a result, the disease is less likely to spread via face-to-face interaction in workplaces.

4.2 Optimal Containment Policy

After showing the role of international trade during the pandemic, the next question concerns the governments' roles in a pandemic. In this subsection, we will discuss the results of optimal containment policies.

[5]The pattern for the total confirmed cases is similar and hence not presented here.

4.2.1 Procedure for Computing Optimal Containment Policies

We first define the policy tool that each government will utilize. Theoretically, the governments of each country could choose a path of containment policies over time. However, the computational burden of finding entire paths of optimal containment policies for all countries is rather heavy. To tackle this problem, we assume governments target effective reproduction numbers. In other words, we assume that each government chooses an effective reproductive number, given other countries' chosen effective reproductive numbers. The government adjusts its containment measures accordingly. The equilibrium we find here is essentially a Nash equilibrium because a country's decision is made given other countries' decisions.

The effective reproductive number is a reasonable target/representation as it reflects the speed of disease spread and is the central concern for epidemiologists and doctors who lead government responses. In addition, targeting an effective reproduction number implies that the containment measures should be stringent initially and gradually relaxed over time, which is in line with a pattern found in several recent studies in the macroeconomic literature focusing on the dynamics of optimal policies in closed-economy contexts; see, e.g., Alvarez et al. (2021) and Jones et al. (2021). This is because the fraction of susceptible people in the population, $S_{i,t}/N_i$, diminishes over time; with a fixed target for $R_{e,i,t}$, this implies that containment measures $\eta_{i,t}$ generally decrease over time, provided that the over-time variability of $R_{0,i,t}$ is modest.

We now describe the procedure for calculating the optimal policies. Specifically, we implement the computations in two steps: we first compute the global uniform policies and then individual countries' policies. Solving in two steps makes it feasible to derive the optimal policy by reducing the computational burden.

In the first step, we consider a simpler problem in which a global social planner chooses an effective reproduction number R_e that applies to all countries such that the global welfare is maximized. Given a chosen R_e, all countries set up their containment policies $\widetilde{\eta}_{i,t}$ to match R_e, whenever possible. Namely, for each country i, $\{\widetilde{\eta}_{i,t}\}_{t=t_i^*}^{730}$ satisfy

$$R_{e,i,t} = (1-\widetilde{\eta}_{i,t})\left[\pi_i^I + \pi_i^L \sum_{j=1}^{J}(1-\mu_i^j)\ell_{i,t}^j\right] \times 18 \times \frac{S_{i,t}}{N_i} \leq R_e, \tag{17}$$

where the equality holds if a positive solution of $\widetilde{\eta}_{i,t}$ exists; otherwise $\widetilde{\eta}_{i,t} = 0$ and the inequality holds. Also, $\widetilde{\eta}_{i,t} = \eta_{i,t}$ for $t < t_i^*$,[6] and $\widetilde{\eta}_{i,t} = 0$ for $t > 730$. The goal of the social planner is to maximize long-run global welfare specified in (15); the optimal solution is denoted as R_e^*. In our simulation, because the economy is solved quarterly and the disease dynamics are solved

[6]Note that it is possible that for those days between January 1, 2020 and the onset of the disease evolution, a country may already adopt containment measures such as border control.

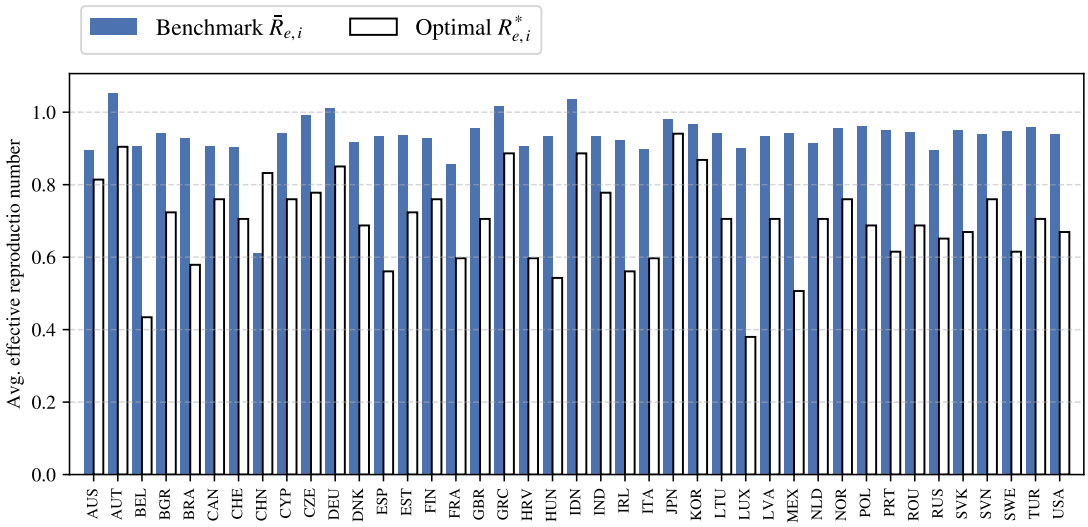

Figure 7: Benchmark Effective Reproduction Number $\bar{R}_{e,i}$ and Optimal Effective Reproduction Number $R^*_{e,i}$

daily, sectoral employment shares $\ell^j_{i,t}$ stay the same throughout a quarter while the containment policies $\widetilde{\eta}_{i,t}$ are updated daily according to (15).

Given the R^*_e calculated in the first step, the second step is to compute each country's optimal policy. The information from the first step is useful for our algorithm of finding a Nash equilibrium of optimal national policies. In particular, we find that the plots of individual countries' welfare against R_e exhibit similar shapes to that of global welfare. Moreover, we find that the effective reproduction number under which the highest welfare for each country is attained is rather close to R^*_e. Thus, these numbers are chosen as the initial guess for the iterations for finding a Nash equilibrium, i.e., a fixed point of best responses (optimal national policies). Given the above findings from the first step, we generally expect that the optimal $R^*_{e,i}$ for each national planner is likely to be found in the neighborhood of the initial guess. Therefore, in our grid search, the grids are much denser in that neighborhood and sparser far away from it. This substantially eases the computational burden. Still, the grid search covers the entire range from a total lockdown to a laissez-faire policy.

4.2.2 Characterization of Optimal Policies

Figure 7 shows the optimal $R^*_{e,i}$ compared with the average effective reproduction number $\bar{R}_{e,i}$ (the over-time average of realized $\{R_{e,i,t}\}$ as reported in Figure 1). We make the following two observations. First, the $R^*_{e,i}$'s for all countries except China are less than their corresponding average effective reproduction numbers in the benchmark model. This means that for all countries except China, the containment measures should be stricter than those actually adopted. Second,

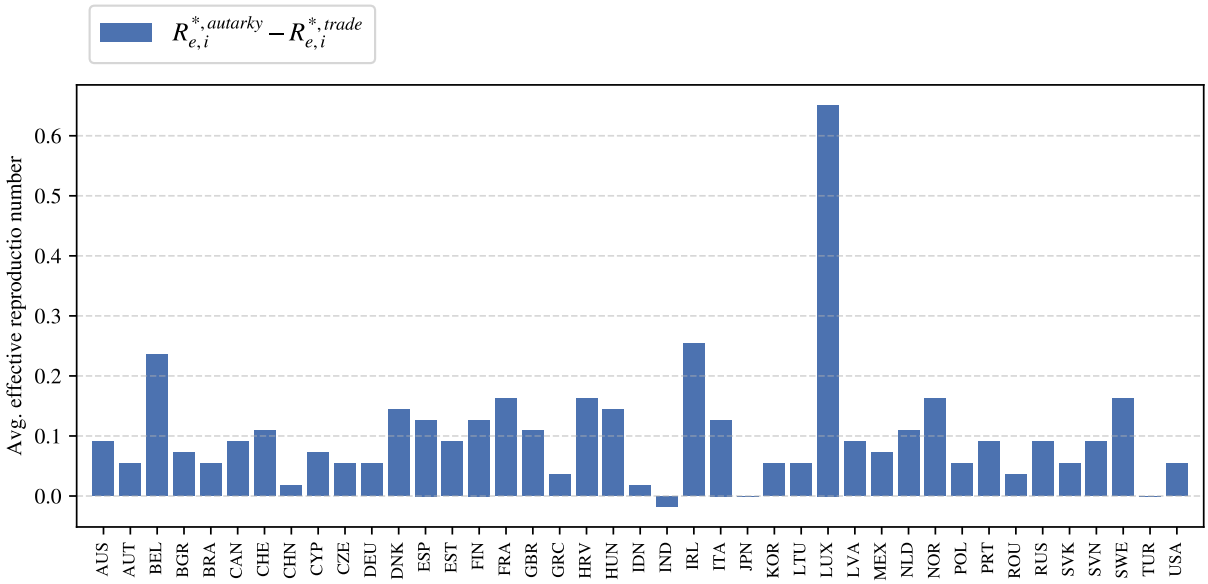

Figure 8: Comparison of Optimal Policies between Trade and Autarky

the optimal $R_{e,i}^*$'s so computed should be interpreted as the upper bounds because we intentionally leave out the psychological cost of mortality. Once this cost is incorporated, optimal effective reproduction numbers should be even smaller; hence the containment measures should be even stricter.

What is the role of trade in optimal policies? To answer this question, we examine how the optimal policies differ in a world where every country is in autarky. Note that this exercise actually computes the optimal policies by simulating the counterfactual case in which each country is in a closed economy. Figure 8 shows the change in optimal $R_{e,i}^*$ when the economy switches from an open economy to a closed economy. A positive (negative) number in this figure means that the optimal containment measure for this country should be more (less) stringent under trade than under autarky. It turns out this number is positive for all countries except India, Japan, and Turkey. This indicates that optimal containment policies are generally tighter with trade than in autarky. To understand this result, note that trade acts as a buffer from pandemic shocks in terms of welfare due to three channels. First, it provides a buffer from real-income losses on average (Figure 4b); second, it smooths consumption paths (comparison between the two panels of Figure 4a and 4b); third, it saves lives (Figure 6). The first two channels are economic benefits, while the third is health benefits. If the third is stronger than the first two combined, optimal policies can be looser. The result indicates that the first two channels actually dominate the third. In other words, trade provides governments with more headroom in terms of economic benefits; hence they can implement stricter containment measures under trade than under autarky.

To further examine the role of trade in terms of the magnitudes of welfare improvements, we

calculate the relative difference in absolute value for each country as follows:

$$\frac{|\text{Welfare Improvement under Autarky - Welfare Improvement under Trade}|}{\text{Welfare Improvement under Trade}}.$$

The average relative difference is 1.47. The corresponding standard deviation for the relative difference is 3.21, indicating large variations across countries. Thus, incorporating trade is both qualitatively and quantitatively important in determining the optimal policy.

One distinctive feature of the containment measures is that they are mostly restrictions on interpersonal interactions, which adversely affect production by curbing the usage of labor. Our model is a full-fledged one that incorporates capital (of which the cross-country differences in ownership account for the trade deficits) and input-output linkages. Both of these reduce the impact of containment measures on the economy. We are interested in learning how much these factors affect optimal containment policies. For this purpose, we simulate the economy and compute optimal containment policies in the following two cases: (1) capital and trade deficits are removed from the model, but input-output linkages are kept; (2) both capital (and hence trade deficits) and input-output linkages are removed.

Table 1: Optimal Policies in Different Settings

	Benchmark	No capital	No capital & No IO linkages
Average $R^*_{e,i}$	0.699	0.853	0.874
Average (weighted) $R^*_{e,i}$	0.777	0.857	0.873

Table 1 reports the cross-country simple average and population-weighted average of the optimal $R^*_{e,i}$ in the above-mentioned two cases and the benchmark case. When the model is reduced to using labor without intermediate inputs or capital, the average $R^*_{e,i}$ is around 0.87, which is much higher than the benchmark case. In the intermediate case where input-output linkages are present but capital is not, the average $R^*_{e,i}$ is around 0.85, which falls between the benchmark case and the case where none of the two factors are present. These indicate that both factors dampen the negative economic effects of the containment measures as they muffle the role of labor, and these dampening effects allow the national planners to impose stricter containment policies. Between the two factors, the results indicate that capital plays a more important role than input-output linkages. While input-output linkages reduce the importance of labor and hence dampen pandemic shocks, they may amplify the negative effect of these shocks because they can propagate these shocks across sectors and countries. This latter countervailing effect of input-output linkages is likely the reason behind the smaller role of these linkages.

4.3 Sensitivity Analysis

In this subsection, we conduct a series of sensitivity analyses to examine how our results in Section 4.1 (the welfare and income losses and the role of trade) are affected by certain key assumptions and parameters.

4.3.1 Input-Output Linkages and Capital

As we have examined the roles of capital (and hence trade deficits) and input-output linkages in determining optimal containment policies, we are also interested in learning how these factors affect welfare/income losses and the role of trade openness. Similar to Table 1, we simulate the case without capital and that without capital or input-output linkages, respectively. The results are shown in the second and third rows of Table 2. To compare with the benchmark (the first row of the table) in order to understand the roles of these factors, it is easier to start from the case with neither capital nor input-output linkages. Comparing the case of no capital with this case reveals the effect of adding input-output linkages to the model. As mentioned in the previous subsection, input-output linkages may either amplify or dampen pandemic shocks. The result indicates that the negative effect that the pandemic shocks are amplified through the input-output linkages dominates the positive effect of the role of labor (and hence containment measures) are dampened due to the presence of input-output linkages. Comparing the case of no capital with the benchmark case reveals the effect of adding capital (and hence trade imbalances) to the model. Here, we see that the welfare and real-income losses are substantially reduced, indicating that capital plays an important role in dampening pandemic shocks by reducing the role of labor. This positive effect of capital is so large that it overcomes the above-mentioned net negative effect of input-output linkages.

Similar to our analysis in Section 4.1, we also examine how much trade acts as a buffer to welfare losses and total deaths. Specifically, the former is calculated as the percentage reduction of the population-weighted average of welfare loss under trade from that under autarky; the latter is calculated as the percentage reduction of global total death under trade from that under autarky. Comparing the second and third rows of Table 2, trade is a slightly better buffer to welfare loss or total deaths when input-output linkages are present. Trade is a better buffer with input-output linkages because countries with severe disease spread and hence stringent containment measures can source both their consumption *and production* from those countries that are less negatively affected. The reduction in domestic production in these countries helps reduce total deaths by reducing workplace transmissions. Comparing the first and second rows, trade is a much better buffer to welfare loss or total deaths when capital is further incorporated

Table 2: Sensitivity Analysis

			Trade as a buffer to	
Cases	Welfare loss (%)	Income loss (%)	Welfare loss (%)	Total deaths (%)
Benchmark	2.34	2.73	11.6	11.7
No capital	4.55	4.58	1.5	9.4
No capital & no IO linkages	4.22	4.44	1.16	9.31
Income support	2.29	2.67	13.4	12.2
No re-infection ($\pi^s = 0$)	2.30	2.69	12.1	11.4
Mortality rate = 1%	2.31	2.71	11.9	12.0
Mortality rate = 3%	2.38	2.76	11.2	11.3
0.9*$R_{0,i}$	2.26	2.66	12.4	4.8
1.1*$R_{0,i}$	2.63	2.99	9.8	10.5

into the model. As the presence of capital reduces the role of labor and hence the negative impacts of containment measures, trade seems to complement this effect to smooth consumption paths (so welfare loss is reduced) and amplify WFH production (so more deaths are avoided) even more.

4.3.2 Income Support Programs

Our benchmark model does not consider income support programs that have been introduced by various countries for those who lost their income due to the disease or containment measures. To examine how our results may be affected by income support programs, we extend the model to allow for such programs; the details of the model and results are provided in Appendix B. Because these programs can be quite complex and vary substantially across countries, an extension accounting for such programs must attempt to capture the essential elements while keeping the model and computation tractable. Our approach is to take advantage of the model feature that an international fund owns capital across the globe. Governments can borrow from this fund to finance their income support measures and must repay the debts during the post-COVID periods. The key idea here is that income support programs may help smooth consumption, but borrowing and lending (instead of free lunches) must be introduced to discipline such programs. There is an income support index from *Oxford COVID-19 Government Response Tracker* that provides a rough measure of the fraction of pre-COVID labor income that is compensated for by the government during the COVID period. We utilize this measure to help account for the cross-country heterogeneity of income support programs.

It turns out that the welfare losses are rather similar between the model with income support

programs and the benchmark model. The long-run real income and welfare do not differ much from the benchmark model as the income support programs are financed by short-term borrowings that need to be repaid during the post-COVID periods. Nevertheless, as we report in Table 2, the weighted average of welfare loss is reduced from 2.34% to 2.29%, while the weighted average of real-income loss is reduced from 2.73% to 2.67%. Despite the slight changes, the income support programs improve long-run welfare and real income because they smooth consumption. Moreover, we see a clear association that the more a country provides support to lost labor income during the COVID period, the more it dampens the welfare loss.

4.3.3 Epidemiology

Third, we consider the sensitivity of key epidemiological parameters. We first experiment with a case where the recovered never lose their immunity and hence there are no re-infections. This is done by setting $\pi^s = 0$. We then gauge how the case mortality rate affects the results by setting $\pi^d = 0.01 \times \frac{1}{18}$ and $\pi^d = 0.03 \times \frac{1}{18}$ (the benchmark is $0.016 \times \frac{1}{18}$). Last, we scale the estimated $R_{0,i}$ up and down by 10%. The results are reported from the fifth to the ninth row, respectively.

When there are no re-infections, we see only slight reductions in both welfare and income losses. It does not greatly affect the importance of trade either. Similar statements can be made regarding alternative case mortality rates. The effects of basic reproduction numbers $R_{0,i}$ are clearly larger. Taken together, the sensitivity analyses on epidemiological parameters indicate that these parameters are not the driving forces for welfare loss, income loss, and the roles of trade, even though they can play an important role in influencing health outcomes and total deaths. One caveat here is that our welfare loss does not incorporate the psychological costs of death; thus our message on welfare loss is less robust. Still, the message on income loss should be robust.

4.4 Discussion

In this subsection, we discuss a few related issues and clarify how this paper should be read from the perspectives of these issues or how the messages of this paper may be influenced.

4.4.1 Vaccines, virus variants, and the uncertainty facing policy makers

First, note that vaccines are difficult to incorporate into the model and calibration explicitly. This is because vaccine rollout differs drastically across countries and because countries also use different combinations of vaccines, the effectiveness of which also differs. Recall that calibrating country-specific infection parameters π_i^I and π_i^L requires simulating the disease dynamics for

each country. From (16), it is clear that the presence of vaccines affects this simulation process by changing the number of people who are susceptible ($S_{i,t}$). Due to the above-mentioned difficulties, it is rather unclear how $S_{i,t}$ is affected by vaccines.

Second, the first batch of vaccines was available around the time when the first dominant variant, the Alpha variant, wreaked havoc on the world. Whereas new dominant variants carry different epidemiological properties from the original strain, their properties are difficult to identify from epidemiological data mainly because the relevant variants co-existed with the vaccines. As the infection parameters are calibrated using the data of total deaths from the beginning of the pandemic all the way up to the end of 2021, this effectively calibrates the **average** epidemiological effects of the original strain, vaccines, and the relevant variants (except the Omicron variant, as explained in Section 3.2). Thus, our model and exercises should be read with the understanding that the calibrated infection parameters reflect the **average** epidemiological effects. Nevertheless, the main goal of this paper is to study welfare and income losses due to the pandemic, the role of trade, and optimal containment policies in an open economy. Our sensitivity analyses on epidemiological parameters show that the qualitative and quantitative results of our main targets are quite robust to these changes in epidemiological parameters, although these parameters may affect health outcomes substantially.

A related issue is that policymakers faced great uncertainty in the early stages of the pandemic. For example, they were still gathering information about the nature of the disease, gauging the prospects of vaccines and potential virus mutations, and examining the policy tools available to them. Admittedly, such uncertainty is assumed away as we assume policymakers know the calibrated epidemiological parameters. In reality, policymakers were obliged to base their actions on educated guesses made by their epidemiologists and doctors. Nevertheless, our sensitivity analyses of epidemiological parameters amount to providing a range of guesses. The fact that the qualitative lessons and quantitative magnitudes of our main targets of analysis remain robust alleviates the concerns regarding the uncertainty facing policymakers.

4.4.2 Trade and international transmission

We have not considered the international transmission of the disease in our model so far. How do the results change if an international-transmission mechanism is incorporated? To answer this, we borrow the theoretical results from Antràs et al. (2023) and contemplate the potential changes. The study by Antràs et al. (2023) connects international trade with international business travel and shows that international trade brings about an externality for disease spread. Depending on the levels of country-specific infection rates and how these rates differ across countries, the externality brought about by international trade can either slow down or accelerate the global

disease spread. In the case where the infection rates are high for most countries, a reduction in trade costs induces a faster rate of infection and accelerates global disease spread. COVID-19 fits this case.

The effect of incorporating this international-transmission mechanism on optimal containment policies is likely ambiguous. First, when international travel accelerates the spread of the disease, optimal containment measures need to be stricter. Second, existing containment measures may dampen both disease spread and trade simultaneously. Since trade brings a cross-country externality on disease spread, containment measures can also become more effective because they depress trade. Thus, optimal containment measures need not be so strict. Based on the above reasoning, we surmise that the inclusion of international travel has an ambiguous effect on optimal containment policies in our framework. If border control is further considered, the above-mentioned externality of trade on disease transmission is reduced, but the ambiguity is likely to remain.

The positive effects of trade on reducing total deaths is dampened if international transmissions brought about by trade are considered. But again, border control or travel restrictions that were once widely implemented when the disease spread was in its most severe phase alleviate the concern due to this countervailing force. Given containment policies, the positive effects of trade on reducing welfare and income losses are dampened only slightly when international transmissions are considered. This is because the effects of having international transmissions are similar to the effects of increasing infection rates. Our sensitivity analyses on epidemiological parameters suggest that such effects on welfare and income losses are slight.

5 Conclusion

The novelty of this paper relative to the literature is mainly two-fold. First, we combine a standard epidemiological compartmental model with a quantitative trade model with multiple countries, multiple sectors, and input-output linkages to evaluate the long-run effects of pandemic shocks and to study the role of trade in these effects. Second, we use effective reproduction numbers as policy targets to reduce the space of candidate policies to study optimal containment policies. Our quantitative analyses prove to be informative; the takeaway messages are as follows.

First, we find that the long-run welfare and real-income losses due to just two years of pandemic shocks are substantial. Second, we demonstrate the importance of international trade, as it helps buffer both welfare and real-income losses. Moreover, it helps save lives. Third, the computed optimal policies indicate that most countries should have tightened their containment

measures relative to what was enacted. Fourth, compared to the case of autarky, the optimal policy under trade is generally more stringent. This is because international trade helps buffer real-income losses such that countries can implement stricter containment measures without significantly reducing real consumption.

References

Acemoglu, D., Chernozhukov, V., Werning, I., and Whinston, M. D. (2021). Optimal targeted lockdowns in a multigroup SIR model. *American Economic Review: Insights*, 3(4):487–502.

Alvarez, F., Argente, D., and Lippi, F. (2021). A Simple Planning Problem for COVID-19 Lockdown, Testing, and Tracing. *American Economic Review: Insights*, 3(3):367–82.

Antràs, P., Redding, S., and Rossi-Hansberg, E. (2023). Globalization and pandemics. *American Economic Review (forthcoming)*.

Argente, D., Hsieh, C.-T., and Lee, M. (2021). The Cost of Privacy: Welfare Effects of the Disclosure of COVID-19 Cases. *The Review of Economics and Statistics*, pages 1–29.

Atkeson, A. (2020). On using SIR Models to Model Disease Scenarios for COVID-19. *Quarterly Review*, 41(1):1–35. Federal Reserve Bank of Minneapolis.

Atkeson, A. G., Kopecky, K., and Zha, T. (2021). Behavior and the Transmission of COVID-19. *AEA Papers and Proceedings*, 111:356–60.

Bonadio, B., Huo, Z., Levchenko, A. A., and Pandalai-Nayar, N. (2021). Global Supply Chains in the Pandemic. *Journal of International Economics*, 133:103534.

Budish, E. B. (2020). Maximize utility subject to $R \leq 1$: A Simple Price-theory Approach to COVID-19 Lockdown and Reopening Policy. NBER Working Paper 28093.

Caliendo, L., Dvorkin, M., and Parro, F. (2019). Trade and labor market dynamics: General equilibrium analysis of the China trade shock. *Econometrica*, 87(3):741–835.

Caliendo, L. and Parro, F. (2015). Estimates of the Trade and Welfare Effects of NAFTA. *The Review of Economic Studies*, 82(1):1–44.

Chen, J., Chen, W., Liu, E., Luo, J., and Song, Z. M. (2020). The Economic Impact of COVID-19 in China: Evidence from City-to-City Truck Flows. Working Paper, Princeton University.

Chernoff, A. and Warman, C. (2022). COVID-19 and implications for automation. *Applied Economics*, 0(0):1–19.

Dingel, J. I. and Neiman, B. (2020). How Many Jobs Can be Done at Home? *Journal of Public Economics*, 189:104235.

Dong, E., Du, H., and Gardner, L. (2020). An Interactive Web-based Dashboard to Track COVID-19 in Real Time. *The Lancet Infectious Diseases*, 20(5):533–534.

Eaton, J. and Kortum, S. (2002). Technology, Geography, and Trade. *Econometrica*, pages 1741–1779.

Eichenbaum, M. S., Rebelo, S., and Trabandt, M. (2021). The Macroeconomics of Epidemics. *The Review of Financial Studies*, 34(11):5149–5187.

Eppinger, P., Felbermayr, G., Krebs, O., and Kukharskyy, B. (2020). COVID-19 shocking global value chains. CESifo working paper.

Fajgelbaum, P. D., Khandelwal, A., Kim, W., Mantovani, C., and Schaal, E. (2021). Optimal Lockdown in a Commuting Network. *American Economic Review: Insights*, 3(4):503–22.

Farboodi, M., Jarosch, G., and Shimer, R. (2021). Internal and External Effects of Social Distancing in a Pandemic. *Journal of Economic Theory*, 196:105293.

Fieler, A. C. (2011). Nonhomotheticity and Bilateral Trade: Evidence and a Quantitative Explanation. *Econometrica*, 79(4):1069–1101.

Gordon, R. J. and Sayed, H. (2022). A new interpretation of productivity growth dynamics in the pre-pandemic and pandemic era US economy, 1950–2022. Technical report, National Bureau of Economic Research.

Hale, T., Angrist, N., Cameron-Blake, E., Hallas, L., Kira, B., Majumdar, S., Petherick, A., Phillips, T., Tatlow, H., and Webster, S. (2020). Oxford COVID-19 Government Response Tracker. *Blavatnik School of Government*.

Head, K. and Mayer, T. (2014). Gravity Equations: Workhorse, Toolkit, and Cookbook. In *Handbook of International Economics*, volume 4, pages 131–195. Elsevier.

Helfand, M., Fiordalisi, C., Wiedrick, J., Ramsey, K. L., Armstrong, C., Gean, E., Winchell, K., and Arkhipova-Jenkins, I. (2022). Risk for reinfection after SARS-CoV-2: A living, rapid review for American College of Physicians practice points on the role of the antibody response in conferring immunity following SARS-CoV-2 infection. *Annals of Internal Medicine*, 175(4):547–555.

Hsu, W.-T., Lin, H.-C., and Yang, H. (2022). Long-run belief-scarring effects of COVID-19 in a global economy. *Available at SSRN 4142920*.

Jones, C., Philippon, T., and Venkateswaran, V. (2021). Optimal Mitigation Policies in a Pandemic: Social Distancing and Working from Home. *The Review of Financial Studies*, 34(11):5188–5223.

Kermack, W. O., McKendrick, A. G., and Walker, G. T. (1927). A Contribution to the Mathematical Theory of Epidemics. *Proceedings of the Royal Society of London. Series A, Containing Papers of a Mathematical and Physical Character*, 115(772):700–721.

Kozlowski, J., Veldkamp, L., and Venkateswaran, V. (2020). Scarring body and mind: The long-term belief-scarring effects of COVID-19. *Jackson Hole Economic Policy Symposium Proceedings*.

Krueger, D., Uhlig, H., and Xie, T. (2022). Macroeconomic dynamics and reallocation in an epidemic: evaluating the 'Swedish solution'. *Economic Policy*, 37(110):341–398.

Low, H. and Pistaferri, L. (2015). Disability Insurance and the Dynamics of the Incentive Insurance Trade-Off. *American Economic Review*, 105(10):2986–3029.

Mayer, T. and Zignago, S. (2011). Notes on CEPII's Distances Measures: The GeoDist database.

Piguillem, F. and Shi, L. (2023). Optimal COVID-19 Quarantine and Testing Policies. *Economic Journal (forthcoming)*.

Ravikumar, B., Santacreu, A. M., and Sposi, M. (2019). Capital Accumulation and Dynamic Gains from Trade. *Journal of International Economics*, 119:93–110.

Sforza, A. and Steininger, M. (2020). Globalization in the time of COVID-19. CESifo Working Paper Series 8184.

Silva, J. M. C. S. and Tenreyro, S. (2006). The Log of Gravity. *The Review of Economics and Statistics*, 88(4):641–658.

Simonovska, I. and Waugh, M. E. (2014). The Elasticity of Trade: Estimates and Evidence. *Journal of International Economics*, 92(1):34 – 50.

Timmer, M. P., Dietzenbacher, E., Los, B., Stehrer, R., and De Vries, G. J. (2015). An Illustrated User Guide to the World Input-Output Database: the Case of Global Automotive Production. *Review of International Economics*, 23(3):575–605.

WHO (2020). Coronavirus disease 2019 (covid-19): situation report, 46.

Appendix

A Quantification

Our model consists of two sets of parameters: economic and epidemiological. We describe how they are calibrated in order.

A.1 Economic Parameters

A.1.1 Risk aversion and time preference

For our quantitative analyses, we set the per-period utility as

$$u(q) = \frac{(q+1)^{1-\sigma} - 1}{1-\sigma}.$$

We choose this functional form for three reasons. First, this specification is similar to the CRRA (constant relative risk aversion) utility if the term $q + 1$ is replaced with q. Thus, it is approximately CRRA when q is large; the parameter σ measures the degree of relative risk aversion. Second, $u(0) = 0$, which satisfies our requirement that psychological costs be left out of the model; note that the exact CRRA utility entails $\lim_{q\to 0} u(q) \to -\infty$ when $\sigma \geq 1$ and is therefore not implementable. Third, $\sigma = 0$ corresponds to the risk-neutral case. Following Low and Pistaferri (2015), the relative risk aversion σ is set to 1.5. Following Farboodi et al. (2021), we set the annual discount rate as 0.95; as daily data is used, $\rho = 0.95^{\frac{1}{365}} \approx 0.99986$.

A.1.2 WIOD

Our main data source is the World Input-Output Database (WIOD), which contains information on bilateral trade for intermediates and for final goods for 43 countries and 56 industries. The country of Malta is dropped as it is not included in the data on containment policy from the Oxford COVID-19 Government Response Tracker. Taiwan is also dropped as its daily COVID cases are zero or close to zero for the entire two years of 2020–2021 except for three months in 2021. This entails the estimates of $R_{0,Taiwan}$ too low to fit the context of an *SIRD* model. Table A.1 lists the 41 countries in the data. We use the data from the year 2014, the latest available year in the WIOD, and aggregate 56 industries into six sectors. See Table A.2 for the list of industries and sectors. Two industries are left out of our aggregation (activities of households as employers and activities of extraterritorial organizations and bodies) since there is no corresponding WFH capability in Dingel and Neiman (2020).

Taking data from the SEA, we proxy country-specific wages by dividing total labor compensation by total employment. Similarly, we proxy country-specific rental prices of capital by

Table A.1: List of countries

ISO-3 code	Country name	ISO-3 code	Country name
AUS	Australia	IND	India
AUT	Austria	IRL	Ireland
BEL	Belgium	ITA	Italy
BGR	Bulgaria	JPN	Japan
BRA	Brazil	KOR	Republic of Korea
CAN	Canada	LTU	Lithuania
CHE	Switzerland	LUX	Luxembourg
CHN	China	LVA	Latvia
CYP	Cyprus	MEX	Mexico
CZE	Czech Republic	NLD	Netherlands
DEU	Germany	NOR	Norway
DNK	Denmark	POL	Poland
ESP	Spain	PRT	Portugal
EST	Estonia	ROU	Romania
FIN	Finland	RUS	Russian Federation
FRA	France	SVK	Slovakia
GBR	United Kingdom	SVN	Slovenia
GRC	Greece	SWE	Sweden
HRV	Croatia	TUR	Turkey
HUN	Hungary	USA	United States
IDN	Indonesia		

dividing total capital compensation by total nominal capital stock. See Timmer et al. (2015). These will be used in calibrating the T_i^j productivity parameters.

Also, from the WIOD, we obtain data on gross production across countries and sectors as well as each sector j's use of intermediates across countries and sectors. The data also include sectoral final consumption across countries. For our model with I-O linkages, we can compute the shares of intermediate use $\gamma_i^{j,l}$ as the shares of total intermediate use by sector j on goods from sector l. The shares of intermediate in gross output, $1-\beta_i^{L,j}-\beta_i^{K,j}$, is calculated by the total intermediate use divided by the gross production. Similarly, the labor share $\beta_i^{L,j}$ and capital share $\beta_i^{K,j}$ are calculated by total compensation on labor and capital divided by gross production. The final consumption shares α_i^j are computed by total sector-j final consumption divided by the total final consumption.

Table A.2: Concordance of WIOD sectors

WIOD description	WIOD code	Industry	WIOD description	WIOD code	Industry
Crop and animal production	A01	Agriculture and mining	Wholesale and retail vehicles	G45	Non-high-skilled service
Forestry and logging	A02	Agriculture and mining	Wholesale trade	G46	Non-high-skilled service
Fishing and aquaculture	A03	Agriculture and mining	Retail trade	G47	Non-high-skilled service
Mining and quarrying	B	Agriculture and mining	Land transport	H49	Non-high-skilled service
Food products, beverages and tobacco products	C10-C12	Food and textile	Water transport	H50	Non-high-skilled service
Textiles, wearing apparel and leather products	C13-C15	Food and textile	Air transport	H51	Non-high-skilled service
Wood and cork	C16	Resource manufacturing	Warehousing	H52	Non-high-skilled service
Paper products	C17	Resource manufacturing	Postal activities	H53	Non-high-skilled service
Printing and reproduction of recorded media	C18	Resource manufacturing	Accommodation and food	I	Non-high-skilled service
Coke and refined petroleum products	C19	Resource manufacturing	Publishing	J58	High-skilled service
Chemical products	C20	Resource manufacturing	Media	J59_J60	High-skilled service
Pharmaceutical products	C21	Resource manufacturing	Telecommunications	J61	High-skilled service
Rubber and plastic products	C22	Resource manufacturing	Computer and information	J62_J63	High-skilled service
Other non-metallic mineral products	C23	Resource manufacturing	Financial services	K64	High-skilled service
Basic metals	C24	Manufacturing	Insurance	K65	High-skilled service
Fabricated metal products	C25	Manufacturing	Auxiliary to financial services	K66	High-skilled service
Electronic and optical products	C26	Manufacturing	Real estate	L68	High-skilled service
Electrical equipment	C27	Manufacturing	Legal and accounting	M69_M70	High-skilled service
Machinery and equipment	C28	Manufacturing	Architectural	M71	High-skilled service
Motor vehicles	C29	Manufacturing	Scientific research	M72	High-skilled service
Other transport equipment	C30	Manufacturing	Advertising	M73	High-skilled service
Furniture	C31_C32	Manufacturing	Other professional	M74_M75	High-skilled service
Repair and installation of machinery	C33	Non-high-skilled service	Administrative	N	High-skilled service
Electricity and gas	D35	Non-high-skilled service	Public administration	O84	High-skilled service
Water supply	E36	Non-high-skilled service	Education	P85	High-skilled service
Sewerage and waste	E37-E39	Non-high-skilled service	Human health and social work	Q	High-skilled service
Construction	F	Non-high-skilled service	Other service	R_S	High-skilled service

A.1.3 Calibrating Portfolio Shares φ_i

We follow the strategy of Caliendo et al. (2019) to calibrate the portfolio shares. First denote D_i as country i's trade deficit, which is calculated directly from the World Input-Output Table for the year 2014. Using data on total capital compensation for each location from the SEA, the portfolio shares are solved

$$\varphi_i = \frac{r_i K_i + D_i}{\sum_{n=1}^{N} r_n K_n}.$$

Since $\sum_{n=1}^{N} D_n = 0$, the portfolio shares satisfy $\sum_{n=1}^{N} \varphi_n = 1$.

A.1.4 Estimation of productivity parameters $\{T_i^j\}$ and trade costs $\{\tau_{i,n}^j\}$

The model's gravity equations and hence trade costs $\{\tau_{i,n}^j\}$ can be estimated given the data on trade shares and geography from the WIOD and Centre d'Études Prospectives et d'Informations Internationales (CEPII). Following Simonovska and Waugh (2014), we set the value of trade elasticity $\theta = 4$. Given trade elasticity, estimated trade costs, various share parameters $\{\alpha_i^j, \beta_i^j, \gamma_i^{j,l}\}$,

and data on wages obtained from the SEA, the productivity parameters $\{T_{i,t}^j\}$ can then be backed out using the model structure. We describe the estimation of trade costs and productivity parameters in order.

Gravity Equation We use a standard approach in estimating productivity parameters $\{T_{i,t}^j\}$ and trade costs $\{\tau_{i,n}^j\}$. Start with the model's gravity equation:

$$X_{i,n,t}^j = \frac{T_{i,t}^j \left(c_i^j \tau_i^j\right)^{-\theta}}{\Phi_{n,t}^j} X_{n,t}^j.$$

Taking the logarithm of both sides, we have

$$\ln X_{i,n,t}^j = \ln[T_{i,t}^j \left(c_i^j\right)^{-\theta}] + \ln[(\tau_{i,n}^j)^{-\theta}] + \ln[X_{n,t}^j (\Phi_{n,t}^j)^{-1}].$$

Assume that trade costs take the functional form below,

$$-\theta \ln \tau_{i,n}^j = \nu_0^j \ln(dist_{i,n}) + \nu_2^j contig_{i,n} + \nu_3^j comlang_{i,n} + \nu_4^j colony_{i,n},$$

where $dist_{i,n}$ is the distance between i and n in thousands of kilometers, and $contig_{i,n}$ equals one if countries i and n share a border. Analogously, $comlang_{i,n}$ and $colony_{i,n}$ indicate whether two countries share the same language and colonial historical links. These variables are obtained from the GeoDist database from the Centre d'Etudes Prospectives et d'Informations Internationales (CEPII) (see Mayer and Zignago (2011)). Thus, the empirical specification is

$$\ln X_{i,n,t}^j = \nu_0^j \ln(dist_{i,n}) + \nu_2^j contig_{i,n} + \nu_3^j comlang_{i,n} + \nu_4^j colony_{i,n} + D_{i,t}^{j,exp} + D_{n,t}^{j,imp} + \varepsilon_{i,n,t}^j.$$

Following Silva and Tenreyro (2006) and Head and Mayer (2014) and using the WIOD data from 2000 to 2014, we apply PPML to estimate the fixed effects model to obtain estimates of $\{\nu^j, D_{i,t}^{j,exp}\}$.

Uncovering Productivity Parameters We follow the trade literature, in particular Simonovska and Waugh (2014), and set $\theta = 4$. Trade costs $\{\tau_{i,n}^j\}$ can be calculated using the estimated coefficients:

$$\hat{\tau}_{i,n}^j = \exp\left(\frac{\hat{\nu}_0^j \ln(dist_{i,n}) + \hat{\nu}_2^j contig_{i,n} + \hat{\nu}_3^j comlang_{i,n} + \hat{\nu}_4^j colony_{i,n}}{-\theta}\right).$$

To best proxy the pre-COVID economy, we use the estimated exporter fixed effects in 2014 in order to back out the pre-COVID productivity parameters T_i^j. Thus, the time subscript is dropped in the following description about how these parameters are backed out. First, observe that

$$\hat{T}_i^j = \exp(\hat{D}_i^{j,exp}) \times (c_i^j)^\theta,$$

where c_i^j is the unit cost of production. As mentioned in Appendix A.1.2, wages w_i and rental prices of capital r_i are observed from the SEA. Hence,

$$\hat{T}_i^j = \exp(\hat{D}_i^{j,exp}) \times \left[w_{i,data}^{\beta_i^{L,j}} r_{i,data}^{\beta_i^{K,j}} (\hat{P}_i^{M,j})^{1-\beta_i^{L,j}-\beta_i^{K,j}} \right]^{\theta} \tag{A.1}$$

$$\hat{P}_i^{M,j} = \prod_{l=1}^{J} (\hat{P}_i^l)^{\gamma_i^{j,l}} \tag{A.2}$$

$$\hat{P}_i^j = \Gamma\left(\frac{\theta - 1 + \kappa}{\theta}\right) \left[\sum_{k=1}^{K} \hat{T}_k^j [w_{i,data}^{\beta_i^{L,j}} r_{i,data}^{\beta_i^{K,j}} (\hat{P}_i^{M,j})^{1-\beta_i^{L,j}-\beta_i^{K,j}} \hat{\tau}_{i,k}^j]^{-\theta} \right]^{-\frac{1}{\theta}}. \tag{A.3}$$

The following procedure is used to solve for $\{T_i^j\}$, as in Fieler (2011) and Ravikumar et al. (2019). Let ξ index the rounds of iterations, and start with an initial guess of $\{\hat{P}_i^{M,j}(0)\}$.

1. Update productivity: $\hat{T}_i^j(\xi) = \exp(\hat{D}_i^{j,exp}) \times \left[w_{i,data}^{\beta_i^{L,j}} r_{i,data}^{\beta_i^{K,j}} \hat{P}_i^{M,j}(\xi)^{1-\beta_i^{L,j}-\beta_i^{K,j}} \right]^{\theta}$.

2. Update sectoral price indices: $\hat{P}_i^j(\xi) = \Gamma\left(\frac{\theta - 1 + \kappa}{\theta}\right) \left[\sum_{k=1}^{K} \hat{T}_k^j(\xi) \left(w_{i,data}^{\beta_i^{L,j}} r_{i,data}^{\beta_i^{K,j}} \hat{P}_i^{M,j}(\xi)^{1-\beta_i^j} \hat{\tau}_{i,k}^j \right)^{-\theta} \right]^{-\frac{1}{\theta}}$.

3. Update the price indices of the intermediate-input bundle: $\hat{P}_i^{M,j}(\xi+1) = \prod_{l=1}^{J} [\hat{P}_i^l(\xi)]^{\gamma_i^{j,l}}$.

4. Stop the iterations if

$$||\hat{P}_i^{M,j}(\xi+1) - \hat{P}_i^{M,j}(\xi)|| < tolerance.$$

   Otherwise, go back to Step 1.

5. Take $\hat{T}_i^j(\xi+1)$ as our new estimates of country-sector-specific productivity parameters.

For the model without input-output linkages, the calibration is the same except that $\beta_i^j = 1$ in (A.1) and (A.3) and that (A.2) is not used.

A.1.5 Work-from-home capacity

To measure WFH capacity by industry, we use the data from Dingel and Neiman (2020), who compute WFH capacity by occupation. We use the data aggregated to the 3-digit NAICS and adopt the version in which each occupation's capacity was manually assigned by these authors by inspecting the definitions of the occupations. Our results remain similar when using the other version, which is algorithm based. The data was downloaded from https://github.com/jdingel/DingelNeiman-workathome.

To calculate each WIOD industry's WFH capacity, we map each WIOD industry to one or multiple 3-digit NAICS industries according to their definitions. Six WIOD industries map directly into two-digit NAICS, in which cases the 2-digit NAICS WFH capacity computed by these

authors are used. When a WIOD industry maps into multiple NAICS industries, we proxy the WIOD industry's WFH capacities by the average across the corresponding NAICS industries weighted by their industrial employment. The industrial employment data is obtained from the Quarterly Workforce Indicators (QWI) under the LEHD program of the Census Bureau (https://ledextract.ces.census.gov/static/data.html); the fourth quarter of 2014 was used as our WIOD data is for 2014. By-industry and by-state employment data is obtained from QWI, and industrial employment is the sum across all states. This procedure creates a $\{\mu^j\}$ for WIOD industries.

In our aggregation of WIOD industries into six sectors, the WFH capacity for each country-sector pair μ_i^j is computed as the average of these capacities across industries in that sector, weighted by the industrial employment in that country as obtained from the WIOD data.

A.1.6 Containment measures

The containment measures $\{\eta_{i,t}\}$ across countries and time are directly obtained from the *Stringency Index* of the Oxford COVID-19 Government Response Tracker (OxCGRT; Hale et al. 2020) at a daily frequency. This index summarizes a government's responses in terms of various closures and containment, including school and workplace closures, stay-at-home requirements, border control, and restrictions on gatherings, public events, public transport, and internal movements, as well as public information campaigns.[7]

A.2 Epidemiological Parameters

The epidemiological parameters to be calibrated are $\{\pi^r, \pi^d, \delta, \pi_i^I, \pi_i^L, \alpha^I, I_{i,0}\}$. As in Atkeson (2020) and several other macro-SIR models, we set

$$\pi^r + \pi^d = \frac{1}{18}\,, \tag{A.4}$$

which means that it takes on average 18 days to either recover or die from the infection.

The case fatality rate is set at $\pi^d = 0.016 \times \frac{1}{18}$.[8] According to Helfand et al. (2022), we set $\pi^s = 0.476\%$.[9] Following Alvarez et al. (2021), we set $\delta = 0.05 \times \frac{1}{18}$. As a WHO (2020) COVID-19 Situation Report indicates that asymptotic and mild cases account for about 80% of the infections, we set $\alpha^I = 0.8$.

[7] For more details, see Hale et al. (2020) and https://www.bsg.ox.ac.uk/research/research-projects/coronavirus-government-response-tracker.

[8] This number is estimated as a case fatality rate. This choice of mortality rate is consistent with our estimation of key parameters using official data on the number of cases as described below.

[9] Helfand et al. (2022) find that for the wild-type and Alpha variant, persons with recent infection had strong protection against symptomatic reinfections for seven months. Thus, we set $\pi^s = 1/210 = 0.476\%$.

For our purpose, it is important to quantify infection probabilities $\{\pi_i^I, \pi_i^L\}$, as they are the key parameters underlying the variations in the rate of disease reproduction across countries, besides economic conditions and containment policies. Also, for the epidemiological evolution to commence, an estimate of $I_{i,0}$ is required (as $S_{i,0} = N_i - I_{i,0}$ and $R_{i,0} = D_{i,0} = 0$); $I_{i,0}$ is generally unknown because the society might be unaware of, unprepared for, or on low alert for the disease, so that the number of the first few reported cases may be quite off. To estimate the country-specific infection parameters $\{\pi_i^I, \pi_i^L, I_{i,0}\}$, we will use non-linear least squares to fit the data of total deaths for each country. Note, however, that calculating total deaths in this global economy where countries are interlinked in various ways as explained in the main text is time-consuming; hence such estimation is infeasible. In particular, the sectoral employment shares $\{\ell_{i,t}^j\}$ are time-varying and determined by the entire vector $\{\pi_i^I, \pi_i^L, I_{i,0}\}_{i=1}^{41}$ for all 41 countries. Thus, the space of candidate estimates is too large to be feasible.

Thus, we adopt a simpler approach to estimate $\{\pi_i^I, \pi_i^L, I_{i,0}\}$ by proxying sectoral employment shares $\{\ell_{i,t}^j\}$ by such shares in the pre-COVID-19 global economy $\{\ell_i^{j,\text{pre}}\}$. Then, the effective reproduction number becomes

$$\begin{aligned} R_{e,i,t} \equiv \frac{T_{i,t}}{I_{i,t}} \times 18 &= (1-\eta_{i,t}) \left[\pi_i^I + \pi_i^L \times \sum_{j=1}^{J} (1-\mu_i^j) \ell_i^{j,\text{pre}} \right] \times 18 \times \frac{S_{i,t}}{N_i} \\ &\equiv (1-\eta_{i,t}) \times R_{0,i} \times \frac{S_{i,t}}{N_i}. \end{aligned}$$

When the disease dynamics are modified this way, the estimation can be done country by country, and the basic reproduction number $R_{0,i,t}$ also becomes a constant $R_{0,i}$. We first estimate the rates of transmission and initial infections, $\{R_{0,i}, I_{i,0}\}$, simultaneously, and then back out infection probabilities $\{\pi_i^I, \pi_i^L\}$.

Let t_i^* denote the first date on which country i's number of total confirmed cases exceeds 50, and assume that the previous day $t_i^* - 1$ is when $I_{i,0}$ is applied. As explained in the main text, we assume that the pandemic ends at the end of 2021, soon after the Omicron variant became widespread. Let T denote December 31, 2021. For each country i, we estimate the following equation using nonlinear least squares:

$$(\hat{R}_{0,i}, \hat{I}_{i,0}) = \text{argmin} \sum_{t=t_i^*}^{T} \left[C_{i,t,data} - C_{i,t}(R_{0,i}, I_{i,0}; \boldsymbol{\eta}_{i,T}) \right]^2,$$

where $\boldsymbol{\eta}_{i,T}$ is the full history of $\eta_{i,t}$ up to date T, $C_{i,t}$ is the number of total deaths at date t from the model, and $C_{i,t,data}$ is the number of total deaths downloaded from the Humanitarian Data Exchange website.[10] This website compiles data from the Johns Hopkins University Center for

[10] Novel Coronavirus (COVID-19) Cases Data https://data.humdata.org/dataset/novel-coronavirus-2019-ncov-cases.

Systems Science and Engineering (JHU CCSE), which documents for COVID-19 the numbers of total cases, total deaths, and daily confirmed cases for more than 200 countries and regions.

Borrowing from the results in Eichenbaum et al. (2021), we assume that $2/3$ of the infections come from general activities. With estimated $\{\hat{R}_{0,i}\}$, $\{\pi_i^I, \pi_i^L\}$ can then be solved from

$$\pi_i^I + \pi_i^L \sum_{j=1}^{J} (1-\mu_i^j)\ell_i^{j,\text{pre}} = \frac{\hat{R}_{0,i}}{18}, \tag{A.5}$$

$$\frac{\pi_i^I}{\pi_i^I + \pi_i^L \sum_{j=1}^{J} (1-\mu_i^j)\ell_i^{j,\text{pre}}} = \frac{2}{3}. \tag{A.6}$$

Note that in our quantitative analyses, the disease dynamics and, in particular, the effective reproduction number $R_{e,i,t}$ are still generated from the full model.

B Income Support Programs

B.1 Model Modifications

This subsection describes how the benchmark model is modified to allow for income support programs in a tractable way. The key idea is to tap into the global fund that owns the capital in all countries as in Caliendo et al. (2019) and allow for borrowing and lending through this fund. While income support programs provide support during the difficult times of COVID shocks and help smooth consumption, borrowing and lending (instead of free lunches) must be introduced to discipline such programs.

Denote country i's pre-Covid income by $w_{i,0}$. Assume that country i can borrow from the global fund to compensate for lost labor income to some extent. Let $V_{i,t}$ be the amount country i borrows from the global fund at time t. Country i's nominal income $Y_{i,t}$ is therefore given by

$$Y_{i,t} = [w_{i,t}L_{i,t} + V_{i,t}] + \varphi_i \left[\sum_{n=1}^{K} r_{n,t}K_n - \sum_{n=1}^{K} V_{n,t} \right]. \tag{B.1}$$

Let υ_i be the fraction of lost real income due to the pandemic shocks that are made up by the government's income support program. Let $\bar{t} \equiv 2022/01/01$. During the COVID period, i.e., $t \in \{1, 2, ..., \bar{t}-1\}$,[11] country i borrows

$$V_{i,t} = \upsilon_i \left[\left(\frac{w_{i,0}}{P_{i,0}} - \frac{w_{i,t}}{P_{i,t}} \right) P_{i,t} \right] \times L_{i,t} \times \mathbf{1}_{w_{i,0}/P_{i,0} > w_{i,t}/P_{i,t}}. \tag{B.2}$$

If $\upsilon_i = 1$, country i's government compensates for the entire shortfall in real wages from the pre-COVID real wages by borrowing from the global fund; if $\upsilon_i = 0$, country i's government does

[11] Recall that the economy module runs quarterly, but here we denote periods daily with the understanding that the situation remains the same across all days in a quarter.

nothing in terms of income support; υ_i can be any number in $[0,1]$. We set $\{\upsilon_i\}$ as the income support scheme across countries.

The borrowing should be repaid after COVID. Assume that the debt is repaid by a fixed perpetual bond payment G_i. The total value of debt is $\sum_{t=1}^{\bar{t}-1} V_{i,t} \times (1+r)^{\bar{t}-t}$, where r is the interest rate. Hence, the perpetual annuity G_i satisfies

$$\begin{aligned}\frac{1+r}{r}G_i =& \sum_{t=1}^{\bar{t}-1} V_{i,t} \times (1+r)^{\bar{t}-t} \\ =& \sum_{t=1}^{\bar{t}-1} \left\{ \upsilon_i \left[\left(\frac{w_{i,0}}{P_{i,0}} - \frac{w_{i,t}}{P_{i,t}} \right) P_{i,t} \right] \times L_{i,t} \right\} \times (1+r)^{\bar{t}-t}. \end{aligned} \tag{B.3}$$

Thus, country i's post-COVID nominal income satisfies

$$Y_{i,t} = [w_{i,t}L_{i,t} - G_i] + \varphi_i \left[\sum_{n=1}^{N} r_{n,t}K_n + \sum_{n=1}^{N} G_n \right]. \tag{B.4}$$

Let $a_{i,t}$ be the transfer to individuals in i at time t; hence the welfare becomes

$$U_i = \sum_{t=0}^{\infty} \rho^t \left[(S_{i,t} + R_{i,t})\, u\left(\frac{w_{i,t} + b_{i,t} + a_{i,t}}{P_{i,t}} \right) + I_{i,t} u\left(\frac{\alpha^I w_{i,t} + b_{i,t} + a_{i,t}}{P_{i,t}} \right) + D_{i,t} u\left(0\right) \right]. \tag{B.5}$$

where the transfer satisfies

$$\begin{aligned} a_{i,t} &= 0,\ t \in \text{pre-COVID} \\ a_{i,t} &= \frac{V_{i,t}}{S_{i,t} + I_{i,t} + R_{i,t}},\ t \in \text{COVID period} \\ a_{i,t} &= \frac{-G_i}{S_{i,t} + I_{i,t} + R_{i,t}},\ t \in \text{post-COVID period.} \end{aligned}$$

B.2 Implementation and Results

In reality, the details of income support programs can be quite complex, and they differ substantially across countries. For our implementation, we utilize the *Oxford COVID-19 Government Response Tracker*, which reports a rough measure of income support for each country in the data set throughout the COVID period. Specifically, the three values of the variable **E1_Income support** indicate that

- $= 0$: no income support
- $= 1$: government is replacing less than 50% of lost salary (or if a flat sum, it is less than 50% median salary)
- $= 2$: government is replacing 50% or more of lost salary (or if a flat sum, it is greater than 50% median salary)

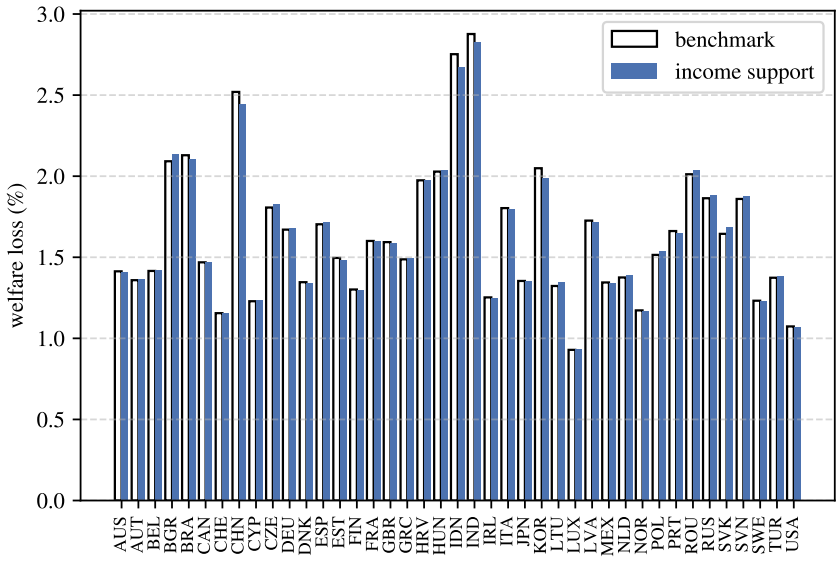

Figure B.1: Welfare Loss with Income Support Programs

Our income support index is calculated as the over-time average of this variable:

$$\upsilon_i = \frac{\sum_{t=1}^{\bar{t}} \left[\mathbf{1}_{\{\text{Income Support}_t=0\}} \times 0 + \mathbf{1}_{\{\text{Income Support}_t=1\}} \times 0.25 + \mathbf{1}_{\{\text{Income Support}_t=2\}} \times 0.5 \right]}{\bar{t}} \tag{B.6}$$

where $t \in \{2020/01/01, \ldots, 2021/12/31\}$. Note that most income-support programs do not last the entire two years of the COVID period that we consider. Also note that for the case where this variable is 2, we assume that the government replaces 50% of lost salary. We take this conservative value because, in reality, not all workers are compensated for the COVID shocks since not all workers are locked away due to WFH possibilities and since many workers are still fully paid due to contractual restrictions. This assumption of 50% is a compromise because while the model assumes that each country i compensates for υ_i fraction of lost labor income *for all workers*, we do not have information on the details of the fraction of workers who are actually compensated in reality.

The interest r is set to $(1-\rho)/\rho$.[12] Figure B.1 reports the welfare losses due to the COVID shocks with income support programs compared with those in the benchmark model. Figure B.2 further reports the difference in welfare loss between the two models, with a positive value meaning more losses are incurred in the model with income support programs than the benchmark model. That is, the difference is $(\text{loss})_i^{\text{income support}} - (\text{loss})_i^{\text{benchmark}}$.

Here, we find that the welfare losses are rather similar between the model with income support programs and the benchmark model. The long-run real income and welfare do not differ

[12] In terms of annual interest rate, $r = 0.0526$ because the annual discount rate is set to 0.95, as mentioned in Section 3.1.

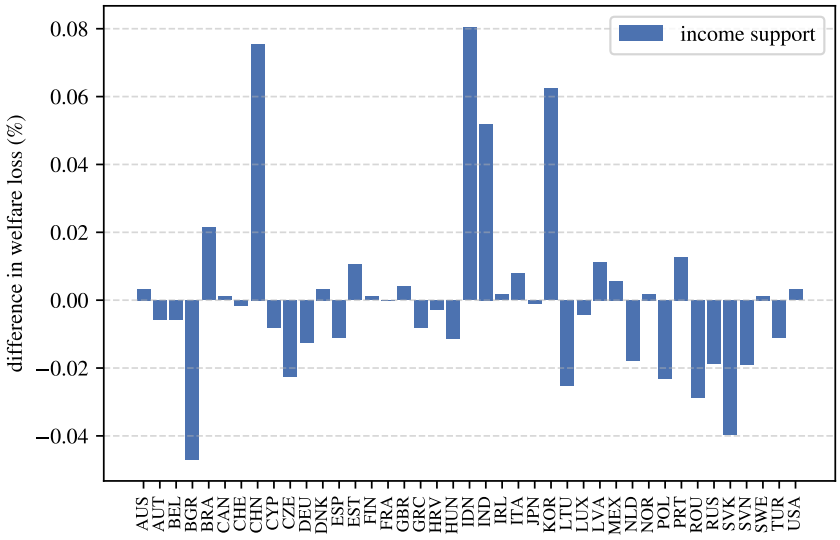

Figure B.2: Difference in Welfare Loss between the Two Models

much from the benchmark model as the income support programs are financed by short-term borrowings that need to be repaid during the post-COVID periods. Nevertheless, as we report in Table 2, the weighted average of welfare loss is reduced from 2.34% to 2.29%, while the weighted average of real-income loss is reduced from 2.73% to 2.67%. Despite the slight changes, the income support programs improve long-run welfare and real income because they smooth consumption.

Finally, Figure B.3 plots the difference in welfare loss as reported in Figure B.2 against the income support index υ_i. Here, we see a clear positive association such that the more a country provides support to lost labor income during the COVID period, the more it dampens the welfare loss. This is consistent with the idea that such programs smooth consumption and enhance welfare.

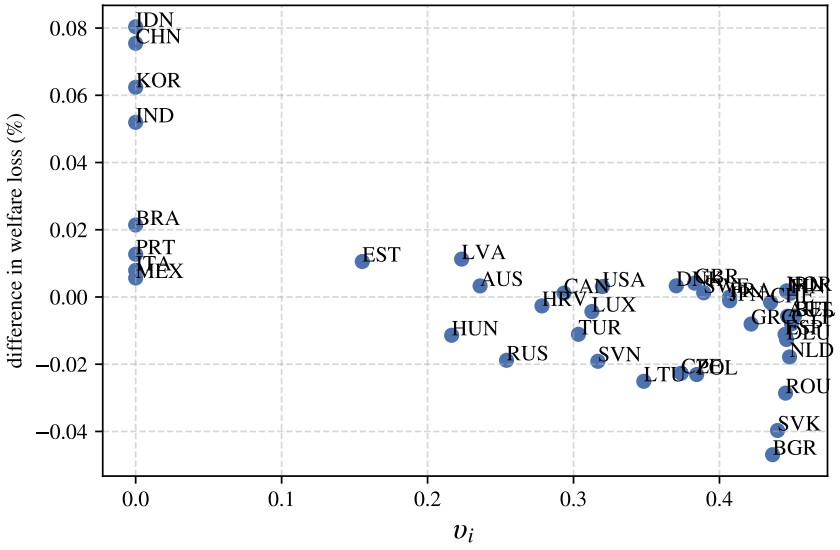

Figure B.3: Differences in Welfare Loss and Income Support Parameter